CHANGE DETECTION IN MULTI-TEMPORAL SAR IMAGES

Oscar López de la Fuente

INDEX

INDEX

ABSTRACT

Change detection in multi-temporal SAR imagery it's a useful tool for preventing natural disasters, studies of the terrain and many other utilities but it's a tool in constant improvement always looking for better results and less computational costs. Though there are many ways to deal with it, the present thesis focuses in change detection using a generalization of the Kittler & Illingworth threshold (GKIT) algorithm which aim is to obtain an unsupervised method for change detection in multi-temporal images. However, the kittler & Illingworth method on his own it's not enough in most of the cases for precise unsupervised change detection. Many factors affect the results. The most significant it's the "speckle" noise, a common multiplicative noise in SAR images. K&I uses a ratio approach to discriminate the "speckle" noise and make it easier to eliminate. As the K&I it's not enough to eliminate the noise many filters are implemented based on wavelet filtering. With two wavelet filtering approaches, based on the discrete wavelet transform (DWT) and on the stationary wavelet transform (SWT), the results are better but still imprecise. The solution to this drawback it's a multi-channel fusion method based on the Markov random fields (MRF). The MRF method fuses filtered ratio images and the original one in order to obtain a final ratio image that eliminates most of the noise retaining most of the details. The use of all this concepts will make a very efficient and precise change detection in multi-temporal SAR images.

INTRODUCTION

In remote sensing, the image data obtained can be of two types, optical images and radar or microwave images. Optical images can only be taken in daytime because they need the radiation of the sun to be taken. They don't trespass clouds and/or smoke (for example the smoke created by a fire in a forest). This kind of images will be useless when the analyzed areas have lots of clouds (rainy days, storms, sandstorms, etc…) or smoke, but in the other hand, these images have very little noise and are very easy to interpret. This is very useful to appreciate details of an area, but with the previous limitations. The second type of images, the radar images, can be taken at any hour, night and day, because the radiation of the sun can be redirected to the specified area through radars. Another advantage is that the radar images can trespass clouds and smoke which is very useful in the cases that optical images can't help. The disadvantage of this images is that they are quite noisy, which makes them difficult to interpret in most of the cases. Either optical or either radar images will be used depending on the situation, the general purpose, the atmospheric conditions or any other aspect of interest. These lines are going to focus only in the last ones, the radar/microwave images.

In the microwave region, one of the most commonly used techniques is side-looking radar. When it uses either an aircraft or a spacecraft it's called SAR (Synthetic Aperture Radar).

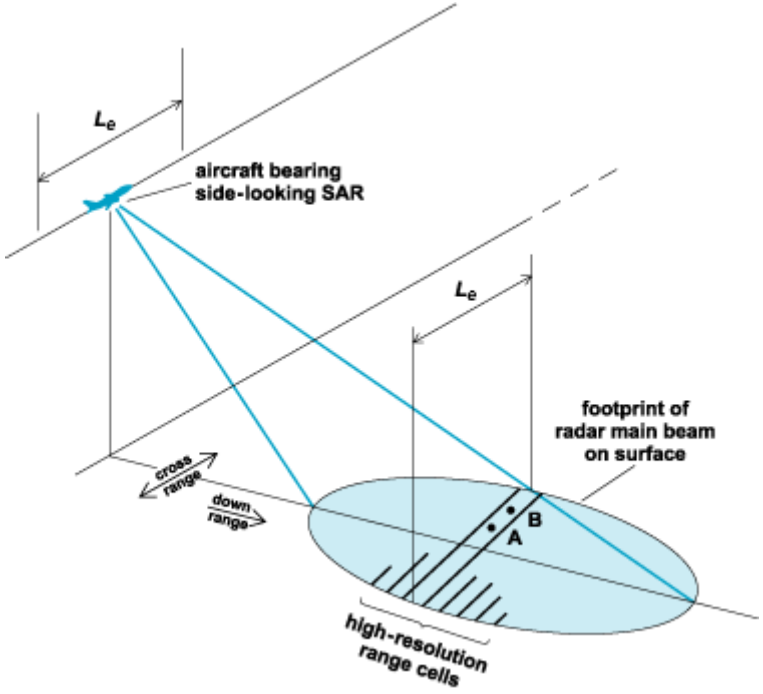

The craft radiates a pulse of electrical energy at the microwave frequency of interest to the earth and then is scattered towards the craft. SAR uses the motion of the craft during transmission of the pulses to give an effectively long antenna, or a synthetic aperture.

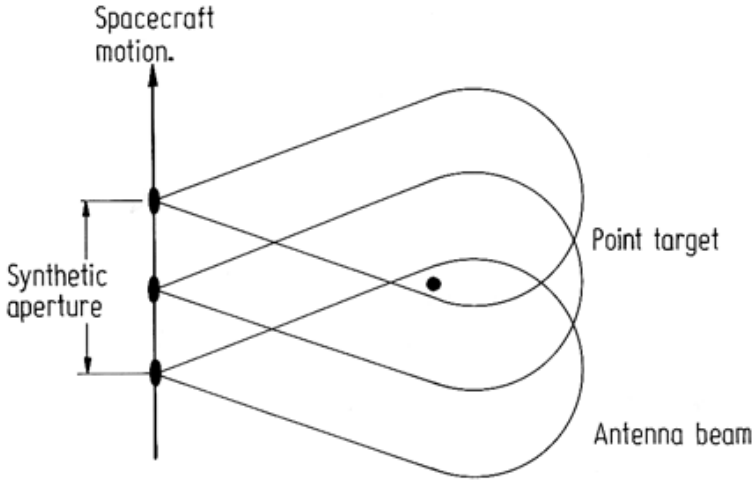

The microwave energy it's measured and the image is formed using the radar principle by using the time delay of the backscattered signals.

In these types of images are going to be detected temporal changes in two images of the same place, but at a different time in which is known something relevant has happened (i.e. natural disasters, cities growth, fields changes, etc….).

There are many ways to deal with multi-temporal SAR change detection but the proposed method operates with image ratioing. This method is an unsupervised change detection method which means no training data to be available at any observation date. In the image ratioing approximation, a ratio image is generated dividing each pixel gray level of one date by the pixel gray level of the other date in the same position. Then the filters can be applied, in order to reduce the noise, and finally one of the proposed generalized kittler & Illingworth methods for change detection.

In change detection, always is needed the best quality in digital images, which means, the biggest amount of information. In SAR Images, the information it's not as accurate as expected and that could difficult the interpretation of the image. The main problem with this type of images it's that they have speckle noise, a granular noise that degrades the quality of the image, caused by the summation of the signals scattered by the ground scatters, that is to say, multiplicative noise, which is more difficult to filter than the additive noise. However there are many ways to reduce the noise.

There have been implemented some methods for noise reduction and better change detection, adaptive smoothing filtering, discrete wavelet and stationary wavelet filtering and MRF (Markov Random Fields) based multisource fusion. The reason for the use of adaptive filters it's due to the nonlinear nature of the SAR images.

For the adaptive smooth filter, is used a binomial filter that will be explained with more detail in the next pages. Before apply this filter (and also the others) a logarithm transform is applied to our ratio image, in order to have a linear image and an exponential transform after applying the filter.

The wavelet filters, both the discrete and the stationary, are a very powerful tool for compressing and image processing. It's also very useful for multi-resolution analysis. The discrete wavelet filter decreases the image resolution $1/2$ with each level applied to degradation, while the stationary wavelet gives many images as

levels applied to degradation but all of them with the same resolution. Thus, the stationary wavelet has more information because the resolution don't change, but it could have a high computational and time cost and sometimes some redundant information, the discrete stationary wavelet it's fast but it's more probably that could be a loss of information in the process.

Even with this filtering change detection in multi-temporal SAR images can be not as accurate as expected or could be a loss of information in the filtering process. Here enters the Markov Random Fields (MRF) theory in which are merged as many images as possible to have the most accurate image possible. In this case, the original ratio image is going to be fused with the filtered ratio images in order to retain as much details as possible but with less noise, which is traduced in better multi-temporal change detection.

In the next pages will be discussed all the previous methods mentioned, the previous work, experimental results and the final conclusions.

STATE OF THE ART

INTRODUCTION:

Remotely sensed imagery of a geographical area of interest represents a precious source of information for many applications (natural disasters prevention, deforestation, land analysis, etc…). The data provided by SAR sensors and his availability provides great potential, because the insensitiveness of SAR to clouds and/or smoke, and other atmospheric conditions. Even more, the short revisit time provided by future SAR missions provides a lot of multi-temporal SAR data to become available. Therefore, multi-temporal SAR imagery is an important tool for disaster prevention and any other ecological applications, especially in change detection techniques between different acquisition dates of an area.

Several approaches have been proposed in the literature to deal with change detection, such as image ratioing, multi-temporal coherence analysis, integration of segmentation with multilayer perceptron and Kohonen neural networks, fuzzy-rule-based analysis, multisource (optical and SAR) and multi-temporal data fusion, spatiotemporal contextual classification, and likelihood ratio tests.

In the image ratioing approach we generate a ratio image dividing each pixel gray level of one date by the pixel gray level of another date in the same position in the image. This is similar to image differencing in optical images. The problem in image ratioing is the criterion for choosing an optimal threshold value for change detection in order to recognize “change” from “no-change”.

In order to automatize the threshold selection, is proposed an unsupervised technique to apply image ratioing with a generalization of the Kittler and Illingworth minimum tresholding algorithm (K&I). The method is modified to image ratioing and the specific non-Gaussian statistics of SAR amplitude ratio images. The developed versions of the generalized K&I threshold (GKIT) have suitable parameter-estimation algorithms based on the method of log-cumulants (MoLC), recently introduced in the context of SAR data modeling.

K&I [1]

K&I assumes a parametric Gaussian model $\mathcal{N}(m_i, \sigma_i^2)$ of a generic single-band image I characterized by the mean m_i and by the variance σ_i^2 for the pdf of a gray level $z_k (k = 1, 2, \dots, N)$ under the hypothesis $H_i (i = 0, 1)$ (H_0 and H_1, "change" and "no change" hypotheses) distinguished by a threshold τ. Denoting pdf by $p_i \cdot m_i, \sigma_i^2$ and the probability of each hypothesis by $P_i = P\ H_i$, K&I turns out the unsupervised threshold-selection problem as the minimization of a criterion function $J(\tau)$ related to the Bayes decision rule for the minimum classification erro (i.e. the "maximum a posterior" (MAP) rule).

Given I_0 and I_1 two equal-sized SAR amplitude images acquired over the same geographical area at times t_0 and t_1, the aim is to detect the changes occurred in the area of interest during the time interval $[t_0, t_1]$. Each image in time t_j will be $I_j = \{r_{j1}, r_{j2}, \dots, r_{jN}\}$ (N being the number of pixels and $j = 0, 1$). In SAR context it's not suitable the classical image differencing, because of the multiplicative "speckle" noise mentioned before. On the other hand, the image ratioing approach prevents undesired effects. This approach generates a ratio image $\mathcal{R} = \{u_1, u_2, \dots, u_N\}$, where $u_k = r_{0k}/r_{1k}$ $(k = 1, 2, \dots, N)$. Once obtained the ratio image $\mathcal{R}$ a decision rule is applied to distinguish quantitatively between one of the two hypotheses.

In order to detect changes in both, a backscatter coefficient increase and a backscatter coefficient decrease, a double threshold should be applied. However, to simplify this operation, a single-threshold approach is adopted. With the mentioned method it's obtained the backscatter coefficient decrease and applying separately the single-threshold to the "reverse-direction" ratio image $\mathcal{R} = u_1, u_2, \dots, u_N$, where $u_k = r_{1k}/r_{0k} = 1/u_k$ $(k = 1, 2, \dots, N)$.

Though, a direct application of K&I to $\mathcal{R}$ is not feasible due to the considerable non-Gaussianity of SAR amplitude ratio data, therefore is needed a generalization of the previous K&I approach. Assuming a parametric model for the pdf of u_k under H_i, three different parametric pdfs are proposed to model the ratio image in the generalized Kittler and Illingworth thresholding algorithm (GKIT). They are based on the Nakagami-Gamma, Weibull and log-normal models for the SAR amplitude images.

Nakagami-Ratio GKIT

The first proposed version of GKIT operates in the context of Nakagami model for SAR, which represents the standard parametric pdf ofr the pixel intensity en the non-textured areas of a SAR multi-look image. This model assumes the SAR images acquired at t_0 and t_1, present a zero complex correlation between each other under each hypothesis H_i. It also assumes they have the same equivalent number of looks. According to the temporal correlation between the images the uncorrelation assumption may result unrealistic. However, this assumption is often accepted as an approximation in the SAR change-detection literature to avoid dealing with more cumbersome conditional parametric models and more complicated parameter estimation procedures.

The proposed estimation technique for the parametric model is MoLC, a parameter estimation methodology based on the generalization of the concepts of characteristic function and moment-generating function by using Mellin transforms. MoLC uses the Mellin transform to finally express the parameter estimation problem as a set of (typically nonlinear) equations. These equations relate the unknown parameters to logarithmic moments or "log-cumulants". In SAR context the method has been proven to be numerically feasible and fast for many SAR-specific models.

In the nakagami-ratio distribution, the parameters are estimated by the MolC method, due to the good theoretical properties before mentioned and the simplicity of the resulting nonlinear equations.

For the K&I parameter estimation are needed only the first two moments and, hence, the first two logarithmic moments of each conditional distribution are sufficient to estimate the Nakagami-ratio distribution.

Log-normal GKIT

The second version of GKIT assumes the amplitude data in the image I_j acquired at each date t_j and conditioned to each hypothesis H_i to be distributed according to a log normal model.

In the log-normal GKIT, the MoLC parameter estimations it's very simple, as the distribution parameters are directly the first- and second-order log-cumulants. This criterion function is very similar to the standar K&I, because the log-normal model can be related to the Gaussian model adopted by the standard K&I by transforming the gray levels according to a logarithmic mapping

Weibull-Ratio GKIT

The third proposed version of GKIT assumes that the amplitudes of the two images are independent and Weibull-distributed with the same values for the shape parameters. As the zero-complex-correlation in the Nakagami-Ratio GKIT, the assumption of equal values for the shape parametes at different dates is a simplifying hypothesis as well. Like the previous GKIT versions, MoLC is adopted as a parameter-estimation strategy.

Once again, like in the Nakagami-ratio model, two parameters are sufficient for the estimation of the Weibull-ratio distribution.

MARKOV RANDOM FIELDS [2]

All the methods addressed before to realize an accurate thresholding for change detection in multitemporal imagery are referred only to single-channel images. Thus, a new classification model is needed for multisource change detection, in order to merge all the data obtained in one image. The basic elements in a multisource classification model are:

- *Input data*. The input images are assumed to be geocoded and co-registered. Image registration involves a transformation of the images to a common map projection. A transformation will

alter the image statistics. If the images contain textured regions or significant noise with known characteristics, then a transformation may be undesirable. If texture is present for only one of the sensors, fusion can be performed in the geometry of this sensor and the classified scene can then be transformed to the desired projection.

- *An image statistic model*. A sensor-specific image statistic model should contain information about the underlying noise characteristics of the sensor and the intrinsic variability of the ground cover classes.

- *Ancillary information*. The backscatter signature for a ground cover measured with a specific sensor normally changes with time and season. Factors such as soil moisture, temperature, wind conditions, and snow cover typically affect the signature.

- *A model for spatial context*. The interpixel class dependency or interpixel feature correlation is modeled for the pixels in a local spatial neighborhood.

- *A model for temporal context*. Temporal context can be modeled for interpixel class dependency or interpixel feature correlation in the same way as spatial context. The ground cover class of individual pixels, in most cases, remains constant over small time intervals. Information about the likelihood of changes with respect to the classes over time for a certain pixel location may provide useful knowledge about the class dependencies. Accurate modeling of temporal interpixel feature correlation for multi-sensor images is difficult. This task requires modeling of the temporal changes in spectral signature for each of the sensors due to different external conditions. A distinction between signature variations due to seasonal changes within the same ground cover class and variations due to an actual change between two classes must also be made. In this paper, we will limit our attention to class dependency constraints.

- *An interaction model*. An essential part of the fusion model is the interaction between the sensor-specific modules, e.g., if fusion is performed at the pixel, feature, or object level.

- *A classification algorithm*. A classification rule must be defined to find a pixel labeling for the scene which is reasonable according to the data and the prior model. This is done by specifying a criterion function or loss function for the scene. An algorithm for optimization of the criterion function is also needed.

- *Parameter estimation procedures*. The parameters of different modules must be specified or estimated. For a complete multisource classification system, parameter estimation procedures should be provided. However, standard techniques for parameter estimation might not be applicable in a complex fusion model.

A methodological framework which allows us to merge all these elements together in a common model is Markov Random Fields. MRF's are frequently used for modeling spatial and/or temporal context. A powerful property of these models is that the prior information and the observed data from different sensors can be easily combined through the use of suitable energy functions. The interaction between the different modules in the fusion model is defined in terms of a sum of sensor-specific energy functions. [2]

As usual in SAR images, speckle noise is always present, in order to reduce it, the use of spatial contextual information it's fundamental. The MRF approach is adopted toward this end. This useful strategy defines suitable "energy functions" and formulates the maximum a posteriori classification criterion as a minimum-energy decision rule model the contextual information in a classification task.

WAVELETS

Wavelet analysis has recently been recognized as a tool with important applications in time series, function estimation, and image analysis. Applications in remote sensing have included the combination of images of different resolutions, image compression, the provision of edge detection methods, and the study of scales of variation. As the development of wavelet methods is recent, the fundamentals are not yet widely understood, and guidance on their

practical use is hard to find. Much of the literature is not easily accessible without much mathematical sophistication.

Wavelets arose from signal processing theory, a signal being the variability of some quantity over time. They can be generalized to two-dimensional signals, of which images are a special case. Wavelet decomposition is an alternative way of presenting the details of a signal which differs from specifying the value of the signal at successive times, the so-called time domain representation.

Other ways of doing this have been used for a long time. The best known is the Fourier series. This represents a signal in terms of sine waves with frequencies which are multiples (harmonics) of a basic frequency. In many applications this is a useful way of decomposing a signal, and its properties can be understood in terms of these oscillations at different frequencies. The sine waves used are orthogonal to each other (two functions $f(t)$ and $g\ t$ are orthogonal if $\int_{-\infty}^{\infty} f\ t\ g(t)\,dt = 0$). For a signal sampled at n points, a full reconstruction can be made from n Fourier components. This is termed the Fourier or frequency domain representation of a series.

A drawback to the Fourier representation is that the frequency components apply to the signal as a whole, and the way that the signal variability changes over time may be important. However, it impossible to say what the frequency components are at a time point, but only in a region about it. To put it another way, a signal cannot be highly localized in both the time and frequency domains (this limitation gives rise in physics to the Heisenberg Uncertainty Principle). One approach is to estimate Fourier components locally, in a set of short intervals, or convolved with a decaying weight function about each point. To do this, however, is to lose the orthogonality and economy of representation of the Fourier method. Wavelets preserve these advantages, while enjoying good spatial and frequency resolution. [3]

While STFT (Short Time Fourier Transform) gives a constant resolution at all frequencies, the Wavelet Transform uses multi-resolution technique by which different frequencies are analyzed with different resolutions.

A wave is an oscillating function of time or space and is periodic. In contrast, wavelets are localized waves. They have their

energy concentrated in time or space and are suited to analysis of transient signals. While Fourier Transform and STFT use waves to analyze signals, the Wavelet Transform uses wavelets of finite energy.

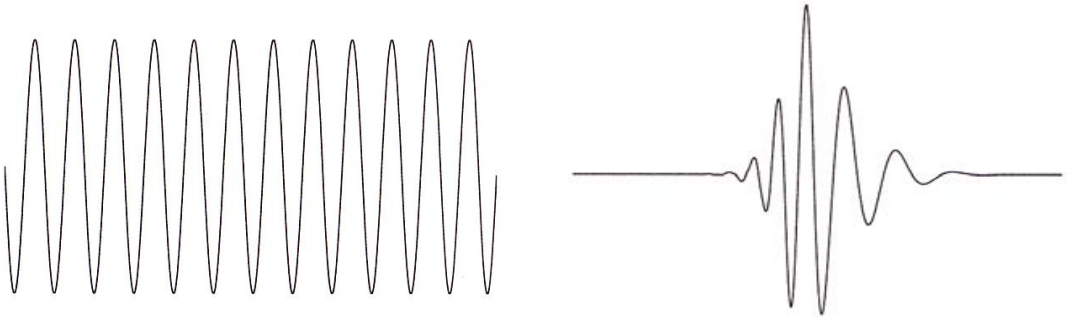

The most important benefits of a wavelet representation are:

- Single wavelet coefficients provide information about how the signal is changing over time: for example, the coefficient of the wavelet which refines the coarsest (overall average) approximation to obtain the next resolution tells us about the overall increase or decrease of the signal.
- Some wavelet coefficients can be discarded (for economy of representation) while still retaining the major features of the signal: this is a form of data compression.
- If one believes that fine details are noise, contaminating the true signal of interest, then discarding or reducing them may give a result closer to the true signal.

There are two main types of wavelet transform - continuous and discrete. Because of computers discrete nature, computer programs use the discrete wavelet transform.

Discrete wavelet transform (DWT)

The Discrete Wavelet Transform (DWT), which is based on sub-band coding is found to yield a fast computation of Wavelet Transform. It is easy to implement and reduces the computation time and resources required. Filters are one of the most widely used signal processing functions. Wavelets can be realized by iteration of filters with rescaling. The resolution of the signal, which is a measure of the amount of detail information in the signal, is determined by the filtering operations, and the scale is determined by upsampling and downsampling (subsampling) operations. The DWT is computed by successive lowpass and highpass filtering of the discrete time-domain signal. This is called the Mallat algorithm or Mallat-tree decomposition. Its significance is in the manner it connects the continuous-time mutiresolution to discrete-time filters.

The process of applying the DWT can be represented as a bank of filters. In case of a 2D image, a single level decomposition can be performed resulting in four different frequency bands namely LL, LH, HL and HH sub band and an N level decomposition can be performed resulting in 3N+1 different frequency bands.

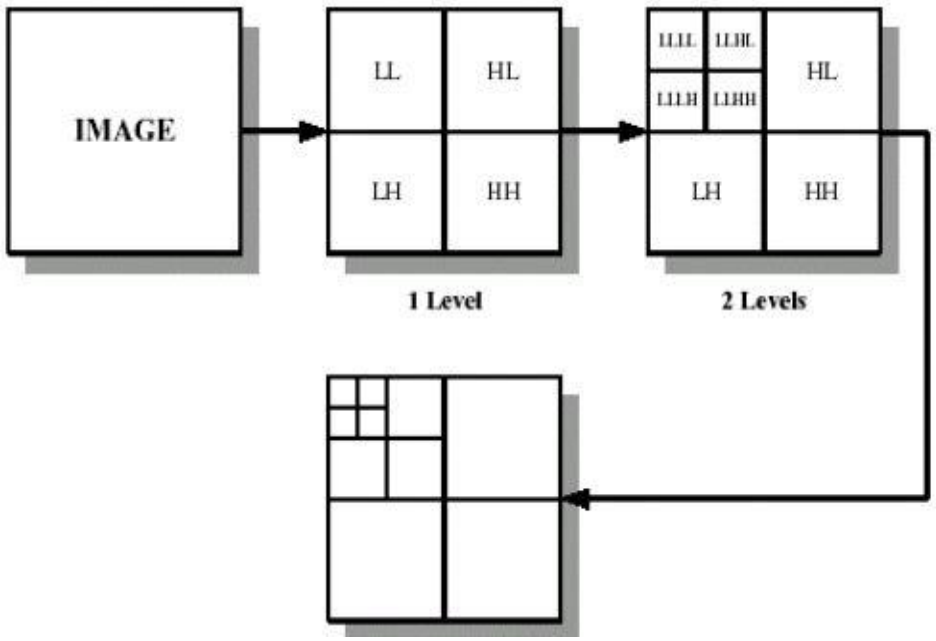

Stationary wavelet transform (SWT)

The discrete transform is very efficient from the computational point of view. Its only drawback is that it is not translation invariant. Translations of the original signal lead to different wavelet coefficients. In order to overcome this and to get more complete characteristic of the analyzed signal the undecimated (or stationary) wavelet transform was proposed. The general idea behind it is that it doesn't decimate the signal. Thus it produces more precise information for the frequency localization. From the computational point of view the SWT has larger storage space requirements and involves more computations.

Applied to image analysis, the image it's not down-sampled with each decomposition level, which means each image of the decomposition is of the same size as the original. This transform it's more cost computational than the DWT and handles many redundant information but the results are more precise because the images are not down-sampled.

PROPOSED METHOD

OVERWIEW

A short and quick approximation of the proposed method is; a filtering algorithm that de-noises multi-temporal SAR images. This task is not quite as easy as it seems, it's necessary to deal with many problems. First, It's not possible to directly apply the de-noise filters to the original images due to the nonlinear nature of the SAR images, hence, an adaptive filter is needed. Besides, applying the filter to the original images will be less efficient and more cost computational than applying it to the ratio image obtained (as said in previous chapters).

The adaptive filter will be an homomorphic filter to convert our non-lineal ratio image into a lineal image by a logarithmic transform. An exponential transform is applied to the filtered image to return the original image properties. All the filters implemented will be smoothing filters to eliminate as much speckle noise as possible. The implemented filters included in the adaptive filter will be:

- Binomial filter: A low pass binomial filter applied to our ratio image. R_0 it's the original ratio image, F_0 the log-transform ratio image, F_1 the filtered image and R_1 the final ratio image.

- Discrete wavelet filter (DWT): Discrete smoothing wavelet filter, it could be any of the wavelet types, therefore, there are many options.

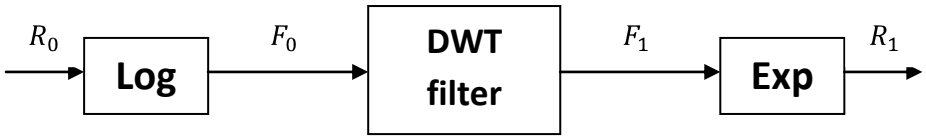

- Stationary wavelet filter (SWT): Stationary smoothing wavelet filter, as in the discrete wavelet filter it could be of any type.

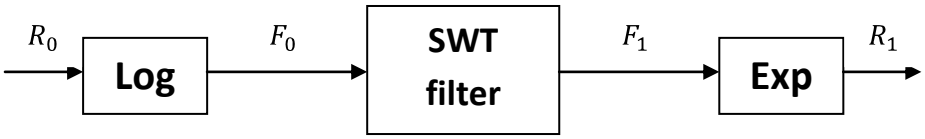

Once filtered the ratio image, it's possible to directly apply the GKIT algorithm to the filtered ratio image, but it's more than reasonable to suppose that has been removed, not only the speckle noise, but some information of the image depending on the smoothing level applied to the ratio image (order level in the case of the binomial filter, and level of decomposition in the wavelet filters).

In order to avoid this loss of information, the solution proposed it's to perform a multi-filtering method and then a multi-channel image fusion using the MRF theory, including all the images filtered and the original one. The proposed method steps are:

1. *Obtain the ratio image*: Using the K&I method described in the previous chapters it's simple to have the coefficient increase and decrease ratio image of the two multi-temporal images.

2. *Apply the chosen filter with different levels*: Once chosen the desired filter, binomial or one of the two wavelet filters (although many different wavelet filters can be chosen), it's applied to the ratio image with many levels as wanted, orders in case of the binomial and decomposition levels in the wavelets case (always doing the logarithmic transform at first and the exponential transform in the end). Therefore, there are as much filtered ratio images as levels applied, plus the original ratio image. All this images are going to be saved in a multi-channel image.

3. *Fuse all the ratio images*: With all the ratio images in one multi-channel image, the next step is to fuse all of them in one single-channel image. The MRF algorithm-based performs this fusion.

4. *Apply the GKIT algorithm*: The final step it's simply to use the GKIT algorithm in the single-channel ratio image to have our two-probability image with the change and no-change classification. Any of the three GKIT models could be used.

The precission of the classification will vary depending, on the filter chosen, the number of levels employed, and in the GKIT model used in the final classification. The block diagram of the proposed method will be:

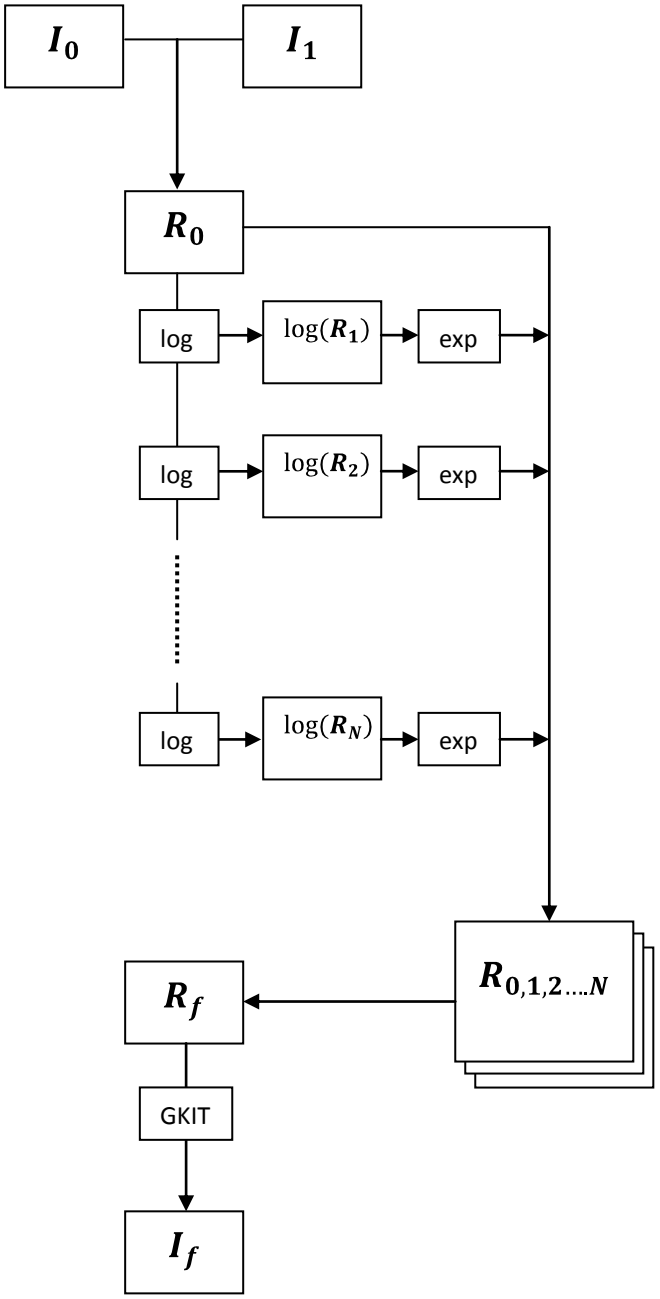

The whole algorithm it's implemented in C++, except for the wavelet filters that are implemented in matlab, due to the simplicity of its toolbox.

FILTER METHODS

Binomial filter

The binomial low pass filter is an approximation of the Gaussian function using the binomial function or the pascal triangle. The binomial function is defined by:

$$f_N = \binom{N}{x} = \frac{N!}{x!\ (N-x)!}\ para\ x = 0,1 \dots N$$

Where N is the desired order of the filter. i.e: for a N=2 order filter, the filter will remain as:

$$f_2(x) = \frac{2!}{x!\ (2-x)!}$$

$$b^2 = f_2(x) = \ 1\ 2\ 1$$

It's easy to obtain looking at the pascal triangle:

$$\begin{array}{ccccccc} & & & 1 & & & \\ & & 1 & & 1 & & \\ & 1 & & 2 & & 1 & \\ 1 & & 3 & & 3 & & 1 \\ 1 & 4 & & 6 & & 4 & 1 \\ 1 & & 5 & & 10 & & 10 \quad 5 \quad 1 \end{array}$$

In which each row corresponds to the order level of the same value of the row, i.e: for the same N=2 order filter, looking at the second row (third in this case because it starts on 0, but it has no sense on applying a N=0 order filter) of the pascal triangle the filter will be:

$$b^2 = f_2(x) = \ 1\ 2\ 1$$

Some of the properties of the binomial filters are:

- They are separated, that is to say, in two dimensions it's possible to apply the same order filter first in the x direction and then in the y direction or viceversa.
- The convolution of a N order filter with itself always gives as a result a 2N order filter.

For image processing is needed a 2-D binomial filter, the filter expression will remain as:

$$b^N = \frac{1}{N^2}\ f_N(x)\ ^T \times \frac{1}{N^2}\ f_N(x)$$

$$b^2 = \frac{1}{4}\ 1\ 2\ 1\ \times \frac{1}{4}\begin{matrix}1\\2\\1\end{matrix} = \frac{1}{16}\begin{matrix}1\ 2\ 1\\2\ 4\ 2\\1\ 2\ 1\end{matrix}$$

The $\frac{1}{N^2}$ it's a normalization factor. Due to the high levels obtained applying this filter the image could alter the luminance and saturate the image. That is the reason why a normalization factor is needed. Pair order filters are used in images for their best resolution properties.

In the case of SAR imagery, as said before, due to the non-linear nature of them, before applying the binomial filter is needed to perform a logarithmic transform to the image and an exponential transform once filtered.

Taking as example this ratio image of the earth-quake of haiti:

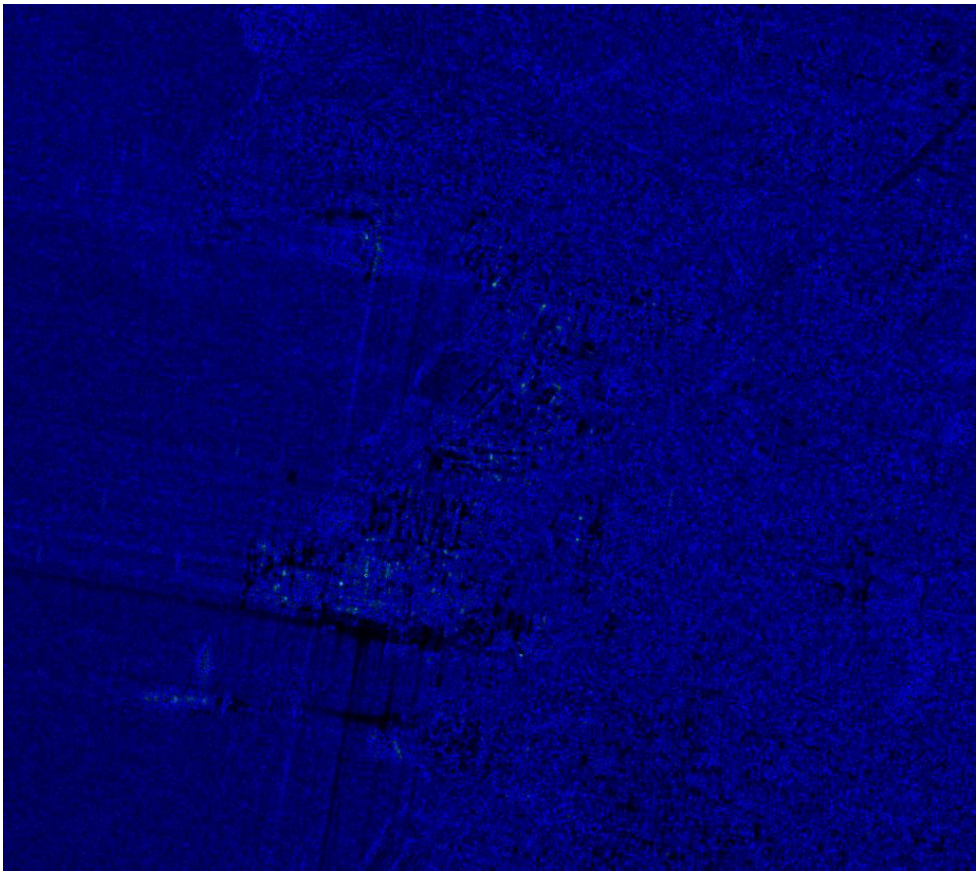

Using the binomial filter from 2 to 8 level order, the resulting ratio images will be:

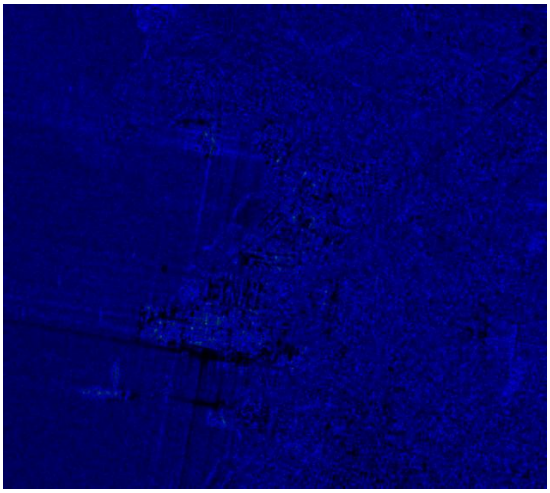

b^2

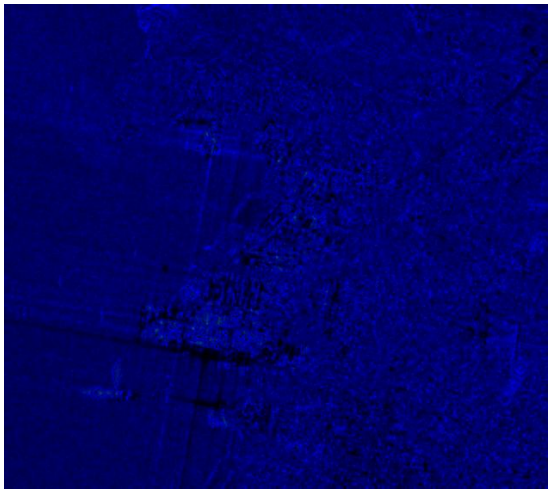

b^4

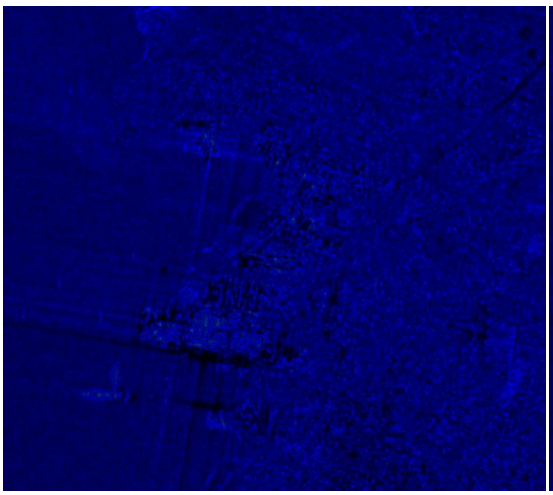

b^6

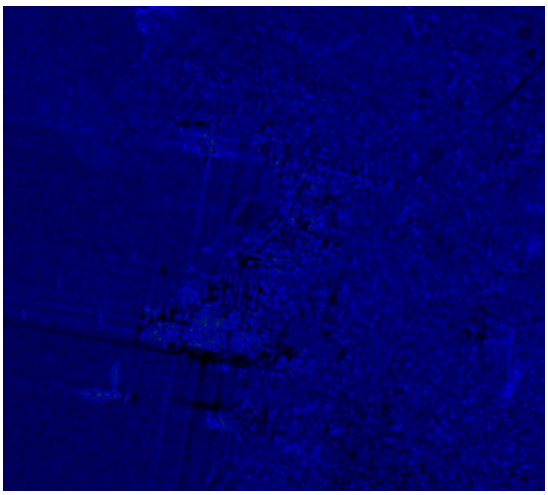

b^8

With the filtered ratio images and the original one is created a multi-channel image with many channels as images. Now, it's possible to fuse all of them in one image with the MRF algorithm that will be explained later. Then, it's calculated the "change" and "no-change" classification using GKIT.

Matlab wavelet toolbox

The wavelet filters parts have been implemented in matlab due to the useful wavelet toolbox that posses, making all the wavelet filtering fairly simple. There is a little explanation of the elements used of this toolbox. Although all the filtering has been code-implemented, it's recommended to know how to use it, because it can be very useful to visualize the expected results or to supervise all the filtering process.

To show the main interface of the toolbox must be written *wavemenu* in matlab (Fig.1).

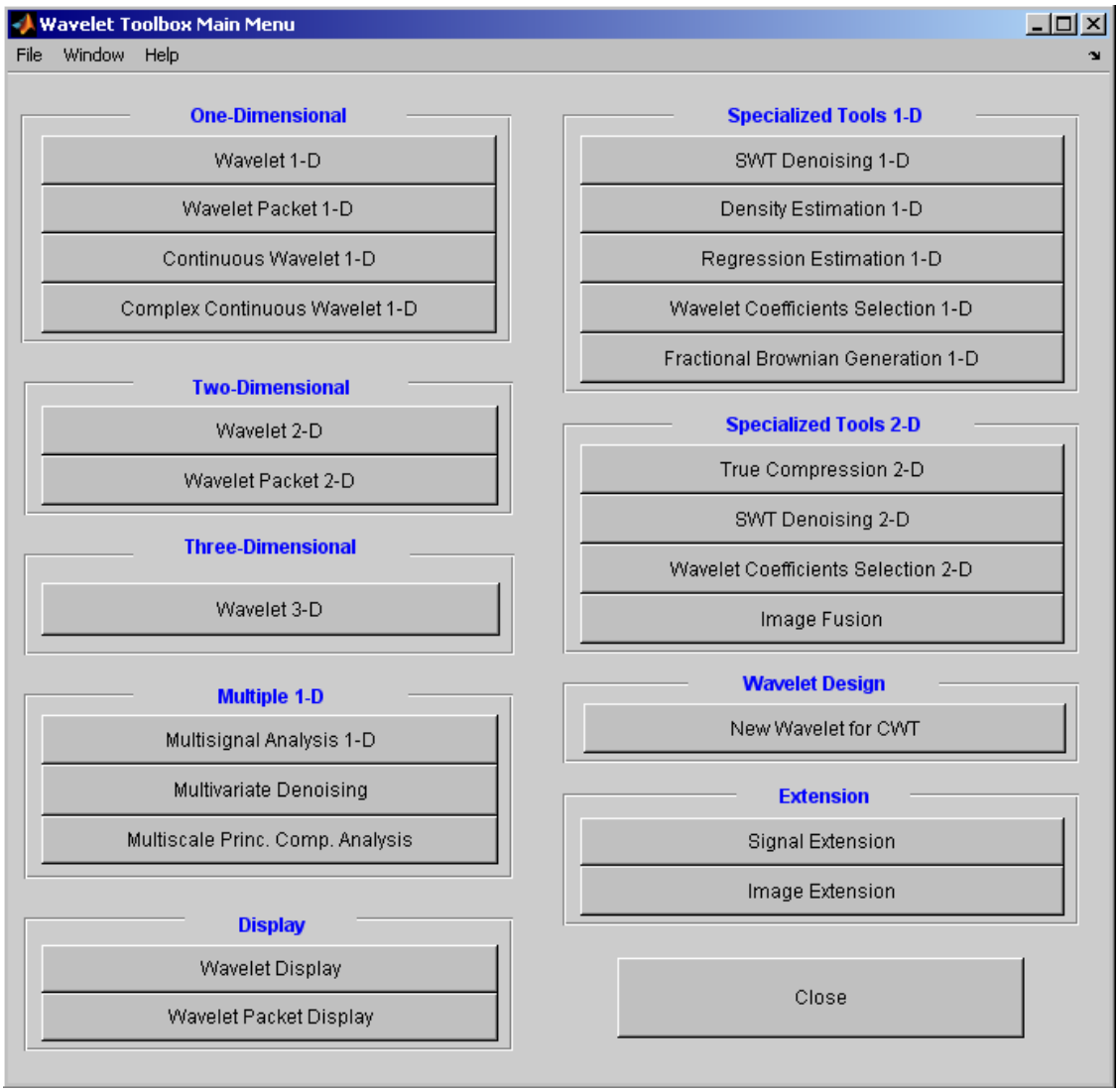

Fig.1: main interface of the wavelet toolbox

In this case, it's used for the DWT, in the 2-D part, the order *Wavelet 2-D* and, in the *specialized Tools 2-D*, the *SWT de-noising 2-D* for the SWT.

Let's start de-noising with the DWT selecting the mentioned button (Fig.2).

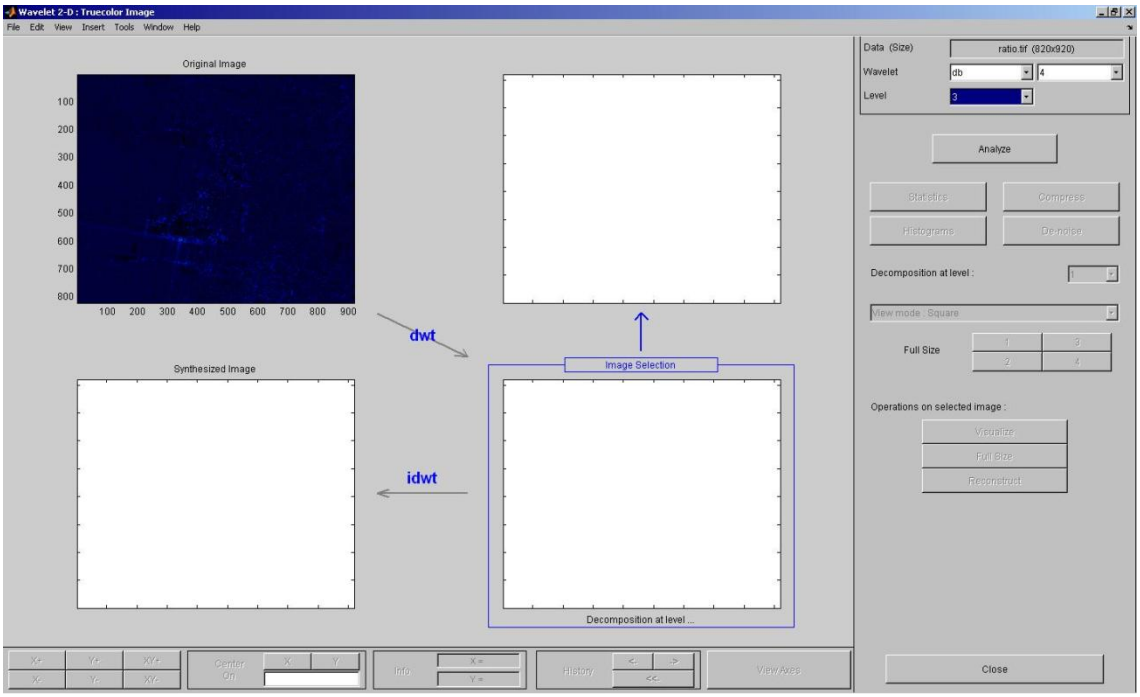

Fig.2: DWT main interface

The steps to de-noise the image are:

- *Load an image*: File->Load->Image
- *Choose a wavelet and its decomposition level*: in the upper right corner are all the options.
- *Click Analyze*: Once clicked the analyze button all the decompositions process is showed and it's possible to visualize each one of the decompositions (Fig.3). There are many more options but there are not important for what we want. i.e: The decomposition of a ratio image with a wavelet db-4 (daubechies) and 3 level decomposition.

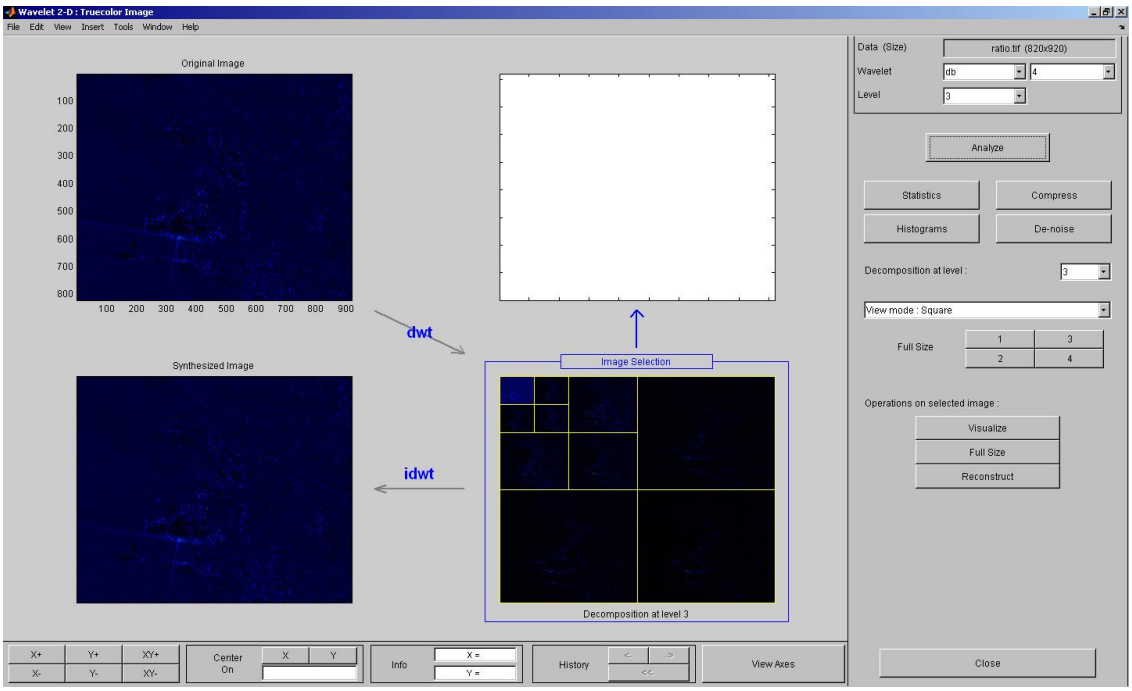

Fig.3: DWT decompositions

- *Click De-noise*: In this interface it's possible to modify all threshold options, and all numeric and graphic values of the side details. To finish, must click the de-noise button again and the de-noised image will show alongside the original image (Fig.4).

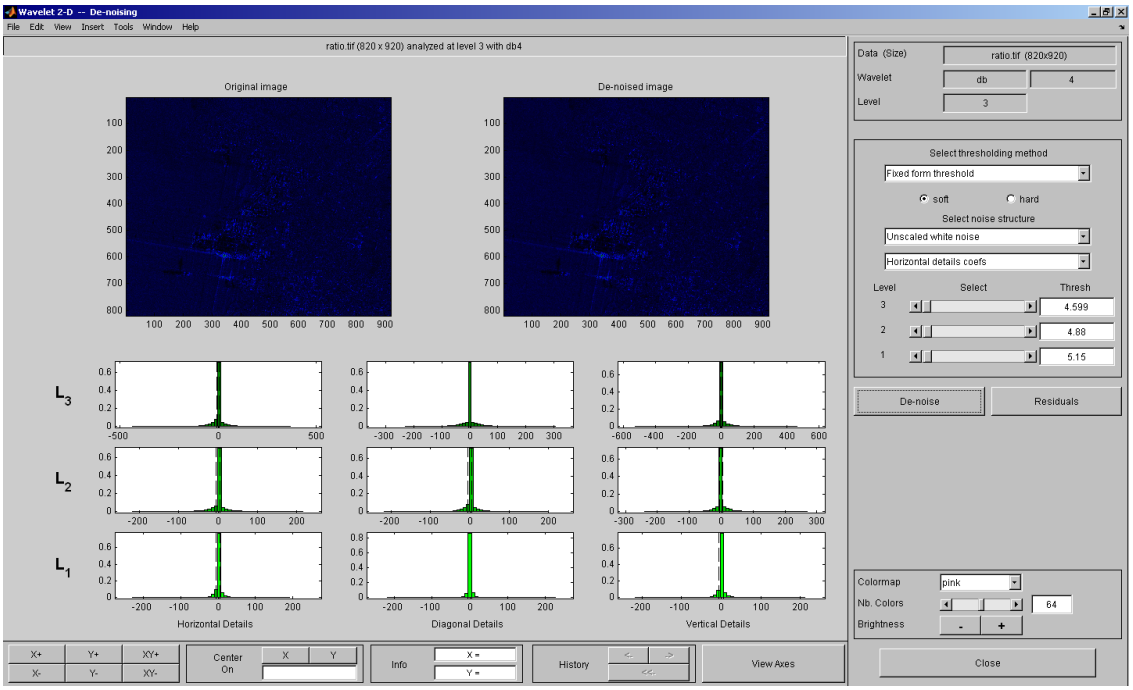

Fig.4: de-noised image

With all the previous steps, it's possible to have the expected experimental result before implement the code, which will help to avoid errors.

For the SWT the interface it's fairly different (Fig.5).

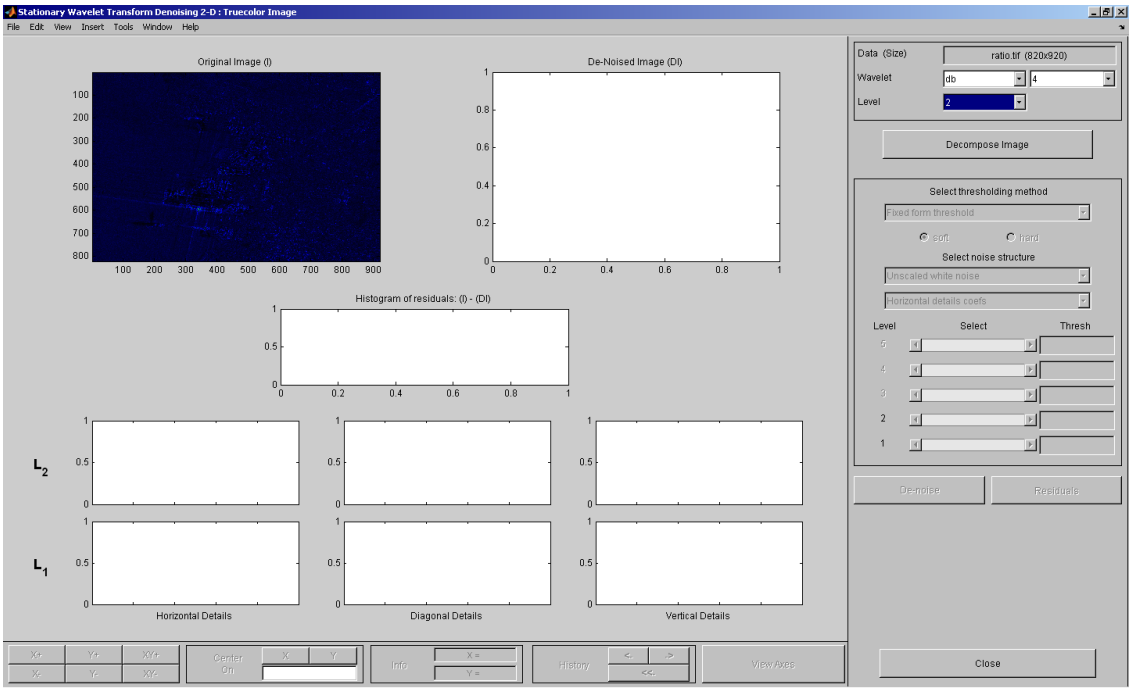

Fig.5: SWT main interface

Again, the steps to de-noise are:

- *Load an image*: File->Load->Image
- *Choose a wavelet and its decomposition level*: in the upper right corner are all the options.
- *Click on Decompose Image*: All side details will be show, however, unlike the DWT, in the SWT interface it's not possible to see the decomposition process.
- *Click De-noise*: Like in the DWT, the de-noised image will appear next to the original (Fig.6).

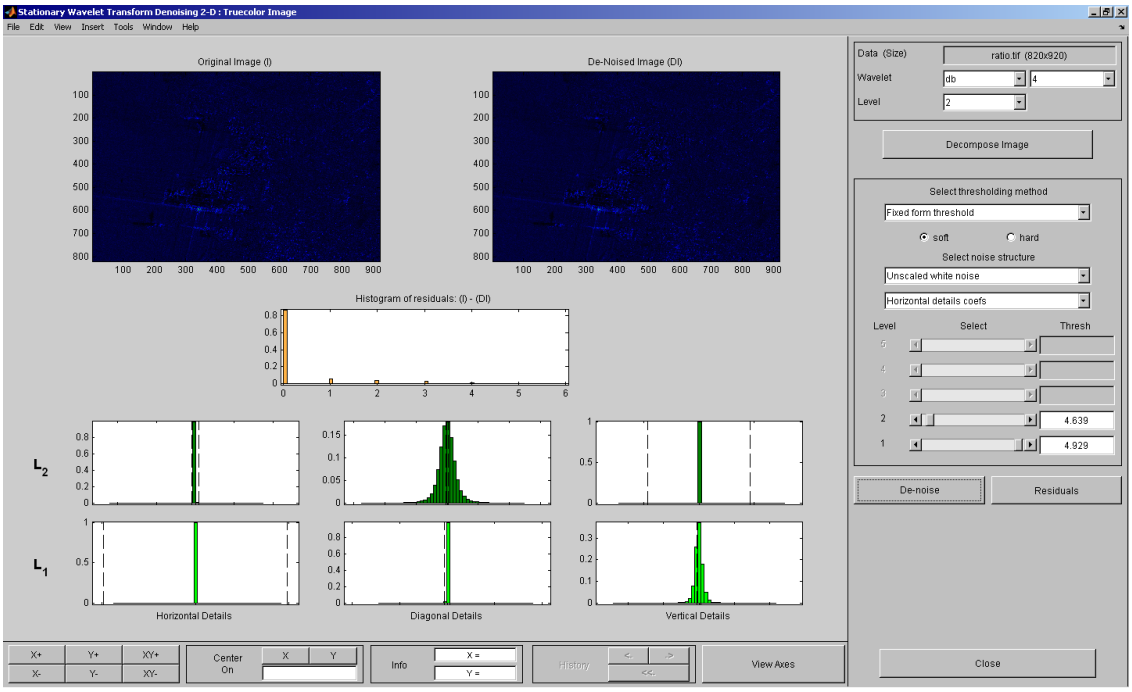

Fig.6: de-noised image

All this simulations, are only oriented for supervision, not for result purposes. All the filtering explained will be code implemented in matlab and the filtered images will be used in the main program in C++.

DWT

As done before with the binomial filter, before filtering a logarithmic transform is needed. The wavelet filtering is quite more complex and more cost computational than the binomial filter, but it's more precise. A simple way to explain the wavelet filtering will be, that, after the filtering, the image it's reconstructed with the horizontal, vertical and diagonal filtered images equal to zero. Doing this, the reconstructed image it's smoothed eliminating most of the noise. DWT re-scale the image each decomposition down-sampling the image $\frac{1}{2}$, that could be a problem if a very precise image is needed because it's easy to lose some information in the reconstruction process. However it's less cost computational than the SWT. The possibilities of the wavelets are many, here are some examples:

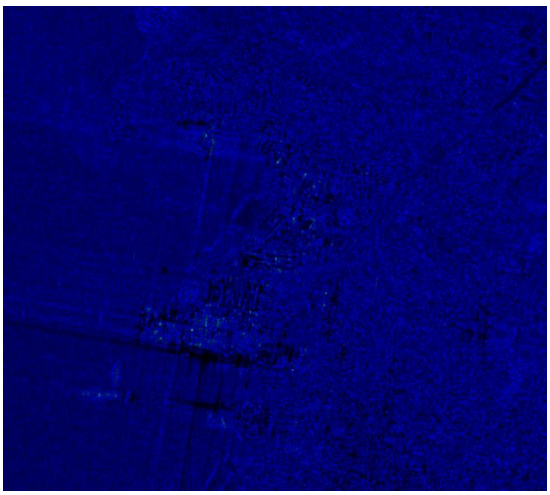

Original ratio image

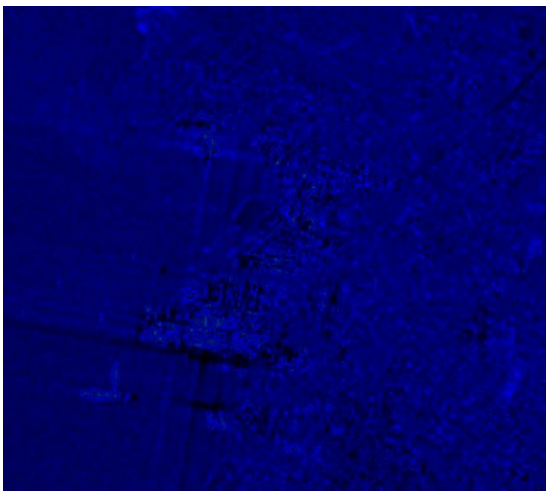

DWT filtering with db-4
(Daubichelies wavelet)

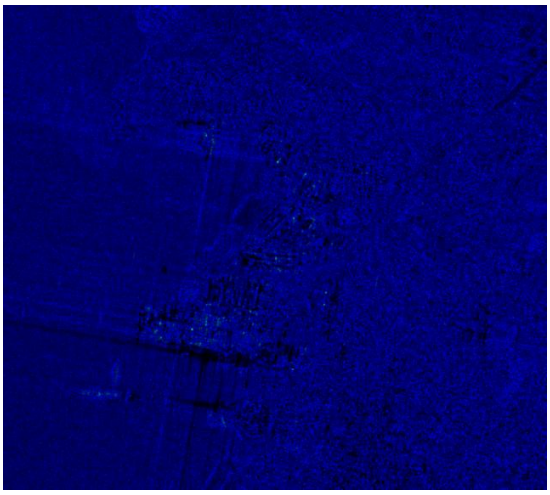

Original ratio image

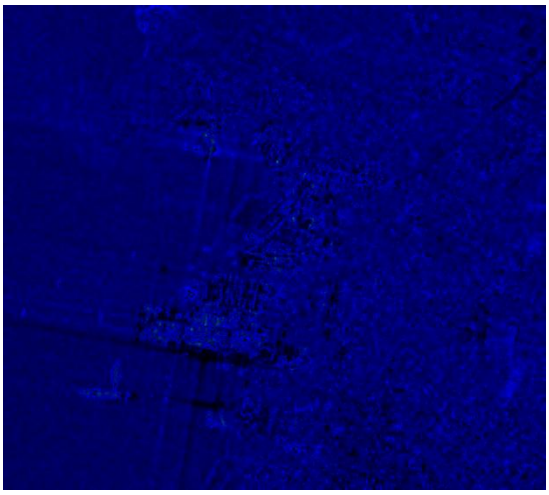

DWT filtering with bior2.4
(Biorthogonal wavelet)

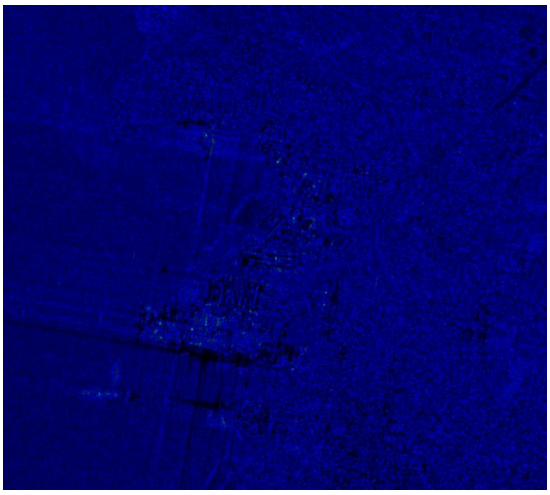

Original ratio image

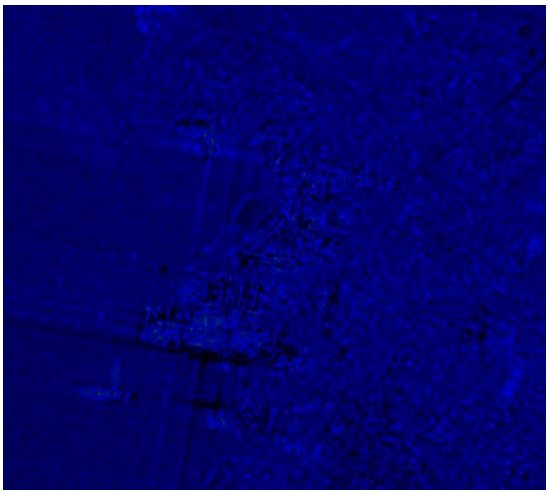

DWT filtering with sym8
(Symlets wavelet)

The wavelet chosen will be selected attending to the needs, but if no specification it's required any wavelet could be chosen.

SWT

As said before, the DWT is very accurate but can lose information in the reconstruction process. The SWT eliminates this drawback not down-sampling the image with each decomposition. Though, higher cost computational is needed.

Like in DWT, de-noise is done by reconstructing the image with all the side filtering images equal to zero, but in this case, all the images have equal size. This method has a lot of redundant information but in the case a high-precision image is needed, this is the recommended method. However SWT has one drawback in matlab; she size of the image must vary to apply higher levels of decomposition. In this case the decomposition level will be limited to 3. The wavelet choose possibilities are still the same as in DWT, here are some examples:

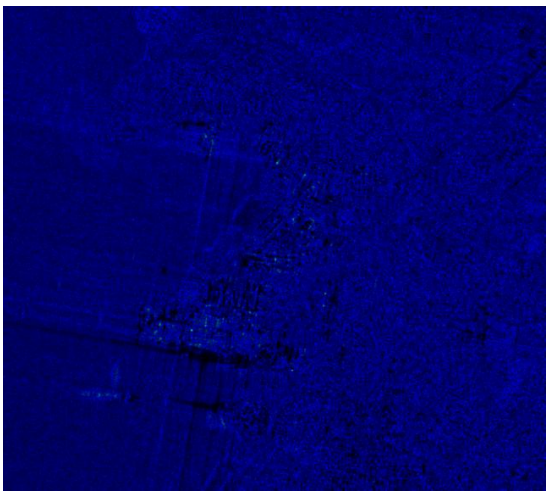

Original ratio image

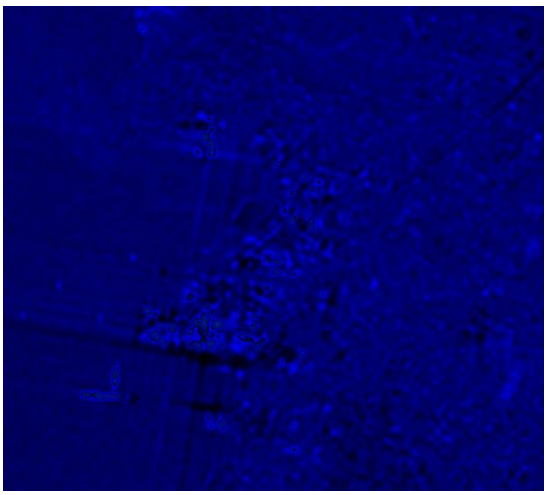

SWT filtering with db-4 (Daubichelies wavelet)

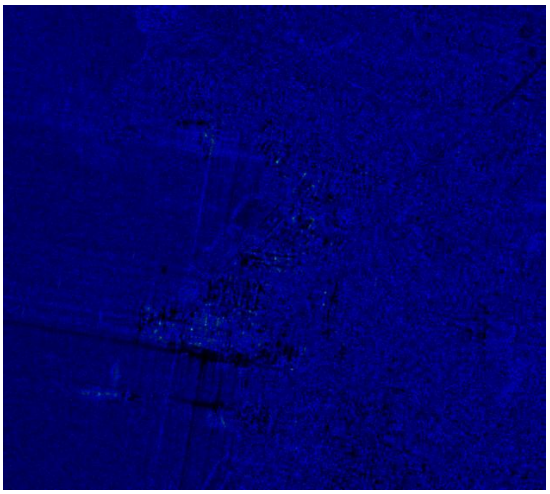

Original ratio image

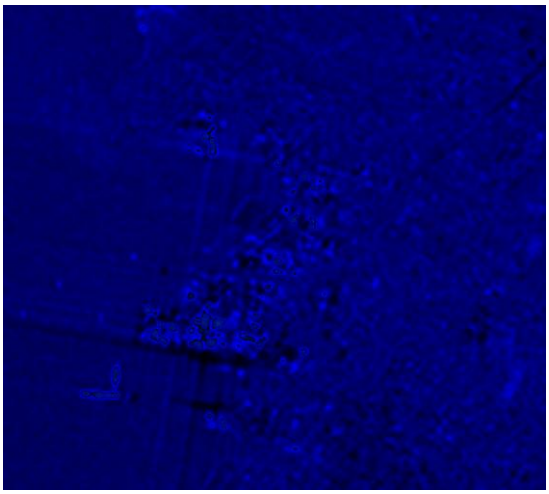

SWT filtering with bior2.4
(Biorthogonal wavelet)

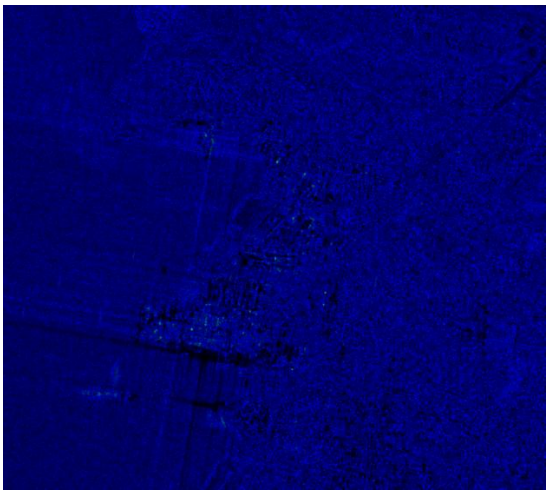

Original ratio image

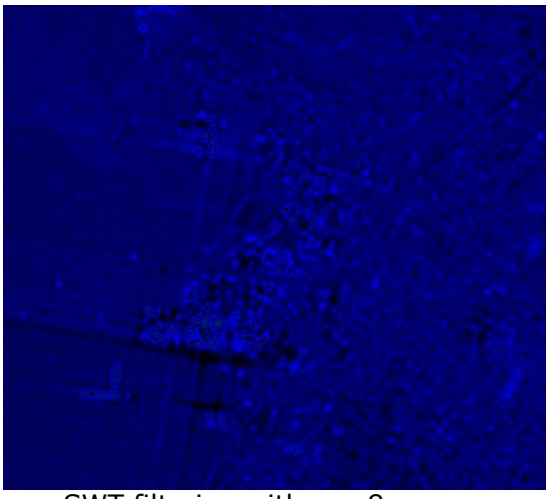

SWT filtering with sym8
(Symlets wavelet)

Any of the wavelets could be chosen if there's not any specification.

MRF [4]

A simple filtering won't work alone. If the filter order is low, it's possible that some noise remains in the image and if the filter order is high, information could be lost. One solution to this drawback is to filter the ratio image with many levels and then, store all of them in addition with the original and fuse all of them with a MRF algorithm.

In his case, two automatic unsupervised change-detection methods, both based on image-ratioing and Markov random fields (MRFs), are proposed for multichannel SAR images. The first technique, combines the EM algorithm developed by Landgrebe and Jackson (LJ-EM) [3] with a SAR-specific version of the Fisher transform. This method, which is denoted as "Fisher-transform-based multichannel change detection" (FT-MCD), is an iterative method and even though a good converge behavior was experimentally observed, no theoretical proof is available yet. The second method proposed overcomes this drawback. It exposes the multichannel SAR change detection problem as a multichannel data-fusion problem. Each SAR channel is considered as a separate information source, and MRFS are adopted for their capability to integrate both the spatial contextual information and distinct information sources into the image classification process. The second technique will be denoted as "Data-fusion-based multichannel change detection (DF-MCD).

The Fisher-transform-based method

Let I_0 and I_1 be two coregistered SAR images, acquired over the same area at times t_0 and t_1, respectively $(t_1 > t_0)$, and consisting of n SAR amplitude channels each. The change-detection problem is formulated as a binary hypothesis testing problem by denoting the "change" and "no-change" hypotheses as H_0 and H_1, respectively. The image-ratioing approach is adopted, that generates a ratio image $\mathcal{R}$ by dividing pixel-by-pixel and channel-by-channel the amplitudes in I_0 by the amplitudes in I_1; hence $\mathcal{R}$ is an n-channel image as well.

The proposed FT-MCD technique represents a modified version of the LJ-EM technique developed for multispectral data. The key idea lies in the application of a SAR-specific version of the Fisher transform in order to compute a (scalar) feature that best discriminates between H_0 and H_1, and in the integration of LJ-EM and MRFs in order to perform a contextual classification in the Fisher-transformed space. The Fisher transform is intrinsically supervised, i.e., it requires training samples for H_0 andH_1, which are not available in the present unsupervised context. To overcome this difficulty, the proposed method employs an iterative approach. It is initialized with the change map generated by the (single-channel) "generalized Kittler and Illingworth thresholding" (GKIT) algorithm, applied to an

automatically selected channel in $\mathcal{R}$. Then, at each q-th iteration $(q = 0, 1, 2, \dots)$, the following processing stages are performed:

- Feature-transformation stage: apply the SAR-specific Fisher transform to the ratio image $\mathcal{R}$ to generate a scalar transformed image F^q by using the current change map M^q as a training map in the computation of the transformation parameters;
- EM-based classification stage: apply an MRF-based formulation of LJ-EM to F^q in order to update the change map (i.e., to generate M^{q+1}).

The technique aims to iteratively improve the change map by generating a sequence of feature transformations, which progressively increase the separation between H_0 and H_1 in the transformed image. The above two stages are iterated until the percentage of pixels with different labels in M^q and M^{q+1} becomes smaller than a predefined threshold (here, equal to 0.1%).

Feature-Transformation Stage

The Fisher transform is a scalar feature mapping that linearly projects a (multidimensional) feature space in an optimal direction, computed by maximizing a functional related to the separation between the sets of samples drawn from two hypotheses (e.g., "change" and "no-change") and to the compactness of such sets. This functional is defined in terms of the sample-means and samplecovariance matrices of the two sample sets; this intrinsically relates the transform to a Gaussian model for each hypothesis.

SAR amplitude ratio data are known to be strongly non-Gaussian. By modeling $\mathcal{R}$ as a set $\{u_1, u_2, \dots, u_N\}$ of n-variate identically distributed random vectors (N being the number of pixels), several parametric models can be used to describe the marginal statistics of the n features in u_k conditioned to $H_i(k = 1, 2, \dots, N; i = 0, 1)$, such as the log-normal (LN), Nakagami-ratio (NR), Weibull-ratio (WR), and generalized Gaussian models.

We adopt a log-normal distribution, since it has already proven effective for single-channel SAR change-detection, and since, unlike

the other mentioned models, it admits a natural extension to the multichannel case, i.e., the multivariate log-normal model. Given H_i such a model is assumed to hold for u_k. Note that, by adopting this monomodal model for H_1, we implicitly focus on the case in which a single typology of change is present in the image.

The transformed image F^q is computed by applying the Fisher transform not to $\mathcal{R}$ but to the corresponding log-ratio image, i.e., by mapping u_k into a scalar feature v_k such that:

$$\ln v_k = \sum_{j=1}^{n} a_j \ln u_{kj} \Rightarrow v_k = \prod_{j=1}^{n} u_{kj}^{a_j}$$

where $a_1, a_2, \ldots, a_n$ are the transformation parameters. Given a training set for H_0 and H_1, a closed-form solution is known for such parameters: as stated before, this training set is replaced here by the sets of pixels assigned to H_0 and H_1 in M^q.

EM-Based Classification Stage

Here, a contextual classification approach is adopted in order to reduce the speckle impact. By denoting as $l_k \in \{H_0, H_1\}$ the hypothesis label of the k-th pixel $(k = 1, 2, \ldots, N)$, the label configuration $\{l_1, l_2, \ldots, l_N\}$ is assumed to be an MRF.

Thanks to the so-called Hammersley-Clifford theorem, one may prove that, if the label configuration is an MRF, then the global maximum a-posteriori (MAP) classification rule (i.e., the maximization of the joint posterior probability distribution of all the N pixel labels, given all the N pixel intensities) is equivalent to the minimization of an "energy function" that is defined only locally, on the basis of the neighborhood. Hence, the intractable global maximization problem involved by MAP allows a tractable local formulation.

According to the minimum-energy MRF decision rule, the generation of homogeneous regions including pixels assigned to the same hypothesis is developed, thus reducing the impact of speckle noise on the classification results.

At the q-th step of FT-MCD, LJ-EM is used to estimate θ and to generate the updated map M^{q+1} (θ is a vector collecting all the model

parameters to be estimated). This technique is an iterative parameter estimation methodology that has to solve problems as data incompleteness and which objective is the maximum-likelihood estimates. EM-type algorithms require long computation times, due they need to do complex computations each iteration.

To overcome this problem, we adopt the "mode-field" approach, which introduces an approximation in the log-likelihood function in order to reduce the computational burden, and which represents a good tradeoff between execution time and classification accuracy.

Each step of FT-MCD, a full cycle of LJ-EM is performed and as a result, M^{q+1} is obtained but, specifically, at the q-th step of the method on the t-th LJ-EM iteration performed the following operations are performed:

1. Compute, for each k-th pixel, the current estimation of the probability.
2. Update the label of each k-th pixel according to the MRF minimum-energy rule.
3. Update the parameter estimates.

LJ-EM is a modified version of the EM algorithm. We recall that EM is known to converge to a local maximum of the log-likelihood function, a similar convergent behavior is expected for LJ-EM as well. LJ-EM is iterated until the differences between the parameter estimates at successive iterations are below a predefined threshold (here equal to 0.001). At each iteration, the parameters of H_i are updated only according to the samples assigned to $H_i (i = 0, 1)$. This aims to compute parameter estimates that reduce the overlapping between H_0 and H_1.

As the initial change map M_0 is generated on a single-channel basis, then, the GKIT technique based on an LN, NR, or WR model for SAR ratio data computes the optimal threshold to a single-channel ratio image by minimizing a "criterion function" defined according to a bayesian approach and related to the probability of error.

The Data-Fusion-Based Method

The DF-MCD technique is still based on a two-hypothesis unsupervised classification of the ratio image $\mathcal{R}$. The keyidea of this method is to model each channel as a distinct information source and to formalize the change-detection problem as a multichannel data-fusion problem addressed by using MRFs. The label configuration $\{l_1, l_2, \ldots, l_N\}$ is assumed again to be an MRF. However, no vector-into-scalar transformations are adopted to map the multivariate ratio vector into a scalar feature. On the contrary, a multichannel fusion strategy is used in order to directly classify in the original multidimensional space.

In accordance with the MRF-based approach to data fusion, the energy function is expressed as a linear combination of energy contributions, each related either to the label configuration or to the information conveyed by each channel of the ratio image. The former is formulated again as a second-order isotropic Potts model and the latter is directly related to the single-variate PDF of the corresponding SAR ratio channel conditioned to "change" and "no-change."

In the case of FT-MCD, the choice of an LN distribution is almost mandatory because the other parametric models proposed for amplitude ratio channels do not admit natural multivariate extensions. For DF-MCD, this constraint does not hold because only the marginal PDFs of the amplitude ratio channels are involved in the MRF model. The NR, WR, and LN distributions are adopted here.

EM-Based Parameter-Estimation and Classification

The proposed DF-MCD change-detection method aims at generating a change map that minimizes the corresponding energy function. Hence, suitable parameter-estimation and classification strategies need to be defined. Toward this end, a case-specific variant of the LJ-EM method is developed by integrating this approach with MoLC.

The application of LJ-EM to the MRF model carries two difficulties. The first, already mentioned with regard to FT-MCD, lies in the computational burden involved by the combination of MRF and EM-type methods and is solved again by adopting the "mode-field"

approach. A further critical point lies in the fact that the maximization problems involved by LJ-EM have no closed-form solutions, when one uses the NR and WR models. In order to address this issue, we propose to combine LJ-EM with MoLC.

LJ-EM is iterative and, as discussed before, when applied according to an LN model, it computes at each iteration, estimates of the conditional logarithmic means and variances. In order to integrate LJ-EM with MoLC in the DF-MDC procedure, is still proposed to update at each iteration, estimates of the conditional logarithmic means and variances as in the LN version of LJEM, and to derive estimates of the distribution parameters by solving the related MoLC equations.

Accordingly, the following operations are performed at the t-th iteration of the DF-MCD algorithm $(t = 0, 1, 2, \dots)$:

1. Compute, for each k-th pixel, the current estimate of the probability.
2. Update the label of each k-th pixel according to the MRF minimum-energy rule.
3. Update the estimates of the spatial parameter and of the logarithmic means and variances
4. Compute, for each hypothesis Hi and each r-th channel, the updated estimate of the parameter vector of the adopted PDF model (i.e., NR, WR, or LN) by plugging the logarithmic mean and variance estimates computed in step 3 in the corresponding MoLC equations.
5. Update the estimate of the reliability factor of each r-th channel.

As in the case with FT-MCD, the procedure is iterated until the differences between the parameter estimates at successive iterations are below a threshold (equal to 0.001). Since the iterative procedure performed by the proposed change detection method is actually derived from EM, a convergent behavior of the method can be theoretically expected.

A single-channel initialization strategy similar to the one employed for FT-MCD is used for DF-MCD, as well, by using GKIT. However, in the case of FT-MCD, GKIT was applied only in its LN

version. Here, it is based on an NR, WR, or LN model, according to the distribution chosen in the energy function. Then, the single-channel change map obtained by applying GKIT to each ratio channel is computed, and the best among such maps is chosen according to the minimum value of the GKIT criterion function and used to define the initial context and to compute the initial parameter estimates.

EXPERIMENTAL RESULTS

DATA SETS

Two 920x280 pixel-sized COSMO-Skymed stripmap images (Fig.1) were used for the experiments. They have been taken from Port-au-Prince (Haiti) in April 26th, 2009, and in January 15th, 2010, with HH polarization and right descending orbit. The second photograph was taken 3 days after an earthquake with an epicenter 15 km from Port-au-Prince. The earthquake reached 7.0 in Richter scale. This earthquake was the most powerful since 1770 in this area with more than 300.000 deaths.

In these images it's going to be tested the algorithm assuming that significant changes will be found, especially in the inhabited areas.

a) **b)**

Fig.1: Images of the zone of Port-au-Prince before **a)** and after **b)** the earthquake.

BINOMIAL EXPERIMENTAL RESULTS

Before focusing in the results provided by the binomial method, it's commendable to see the experimental results of the GKIT method without any filtering and any multi-channel fusion image procedure, in order to visualize the improvements of the methods. It's also important to remark that there is not being calculated any numeric or quantificable data for now. All the results are subjective, images that must be judged by the observer in function of his needs. However, the results and the improvements are obvious.

Every time the whole algorithm is performed, three final images are obtained; the first one called *ChangeMapForward*, corresponding to the increase of the radar backscattering, the second one *ChangeMapBackward*, corresponding to the decrease of the radar backscattering, and the last one *ChangeMapOr*, which is simply the result of applying a logical operator *or* to the two previous images (Fig.2). The colors used in the final images to difference the "change" from the "no-change" conditions will be, black and green respectively in order to appreciate better the two conditions. This color declaration has nothing to do with the originals and it's not a standard, the election of colors rests finally in the supervisor, programmer or observer.

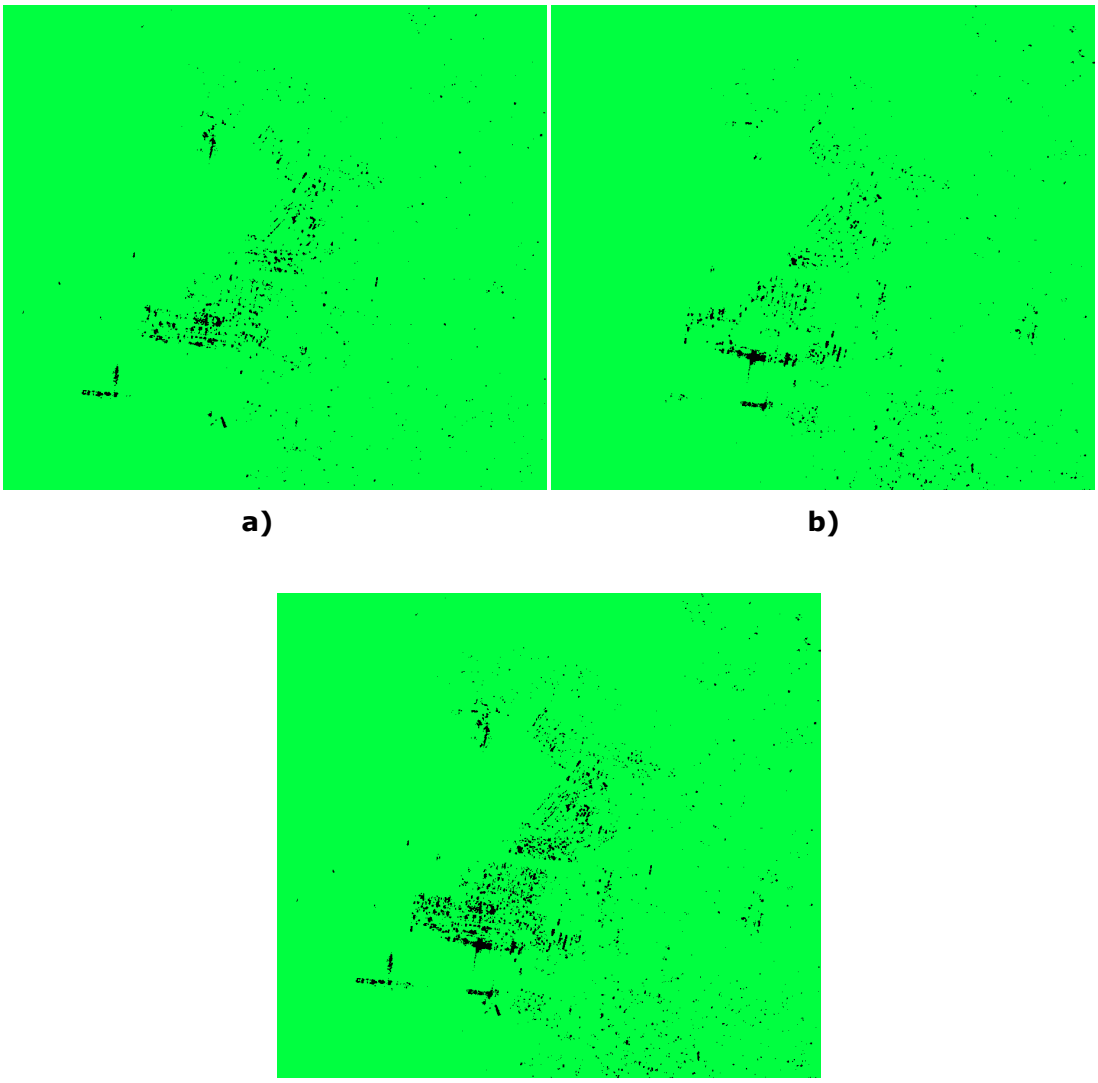

a) **b)**

c)

Fig.2: Comparison between the three final images obtained, the *ChangeMapForward* **a)**, the *ChangeMapBackward* **b)** and the *ChangeMapOr* **c)**.

In order to simplify the comprehension, and to avoid an overbooking of images, in the next methods will be only analyzed the *ChangeMapForward* image, assuming that the other two will suffer analogue changes.

First of all, it's easy to demonstrate that only filtering, the results are not worthy enough as we see in the next example, using only a 4-th order binomial filter (Fig.3).

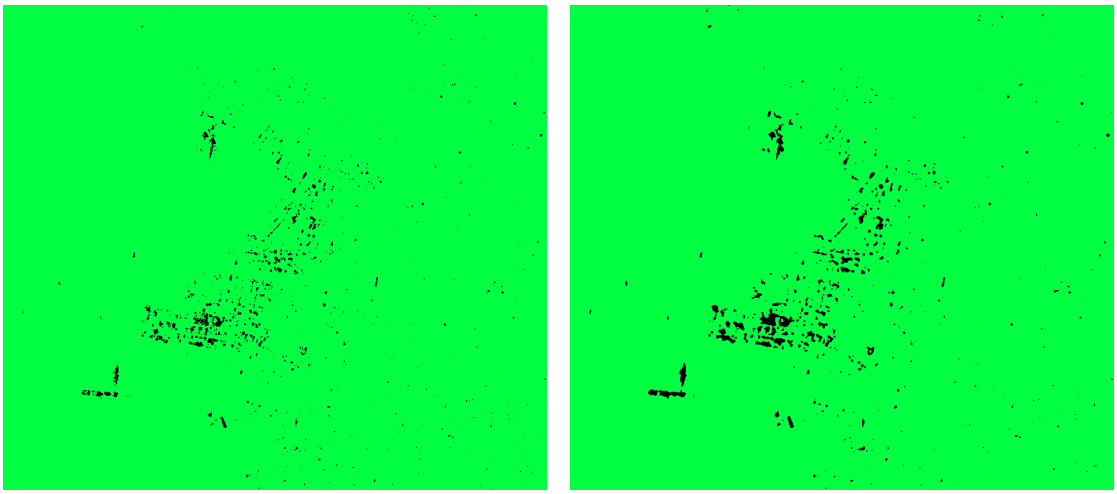

a) **b)**

Fig.3: Final image without any filter **a)** and with a 4th order binomial filter applied to the ratio image **b)**.

There aren't significant differences between both. To appreciate changes it's necessary to apply the multi-filtering process explained in the previous chapters.

In the next image it's applied the whole algorithm with a 2-th and 4-th order binomial filtering to the ratio image and fused both with the original ratio image.

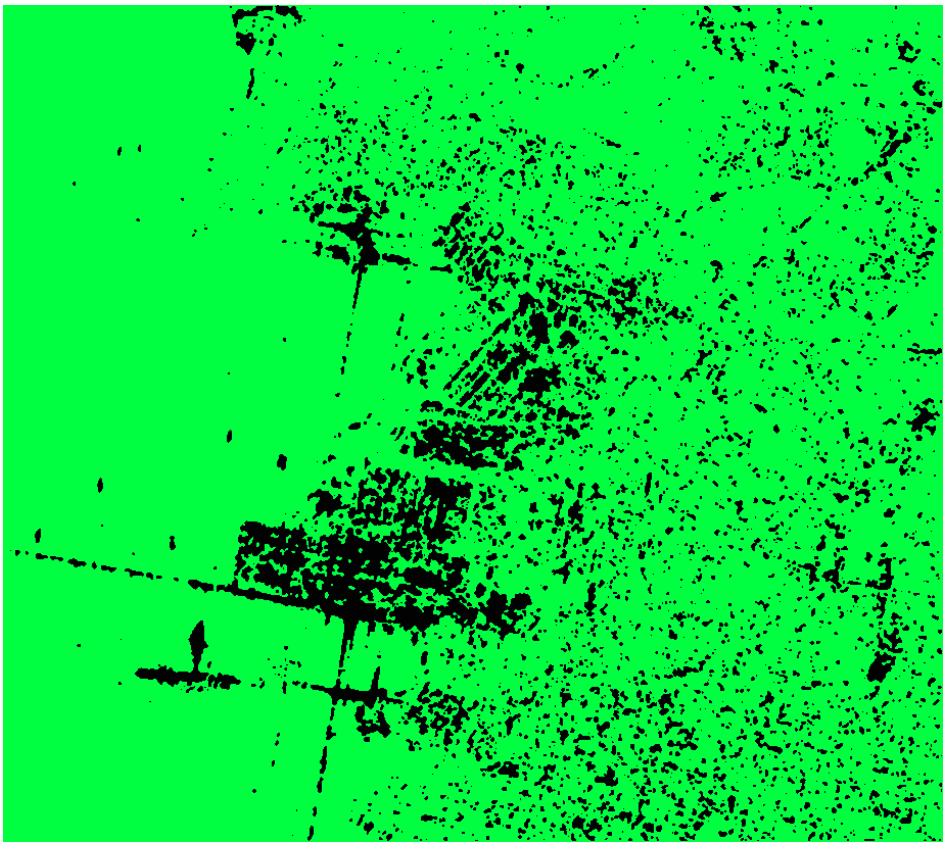

2nd and 4th order ratio image fusion

As mentioned before the changes are obvious and the program detects quite a lot more “change” decisions.

This increase of information will be more accurate if more filters are applied, and with this method, proposed as multi-channel, it’s easy to check how the final images increase their accuracy.

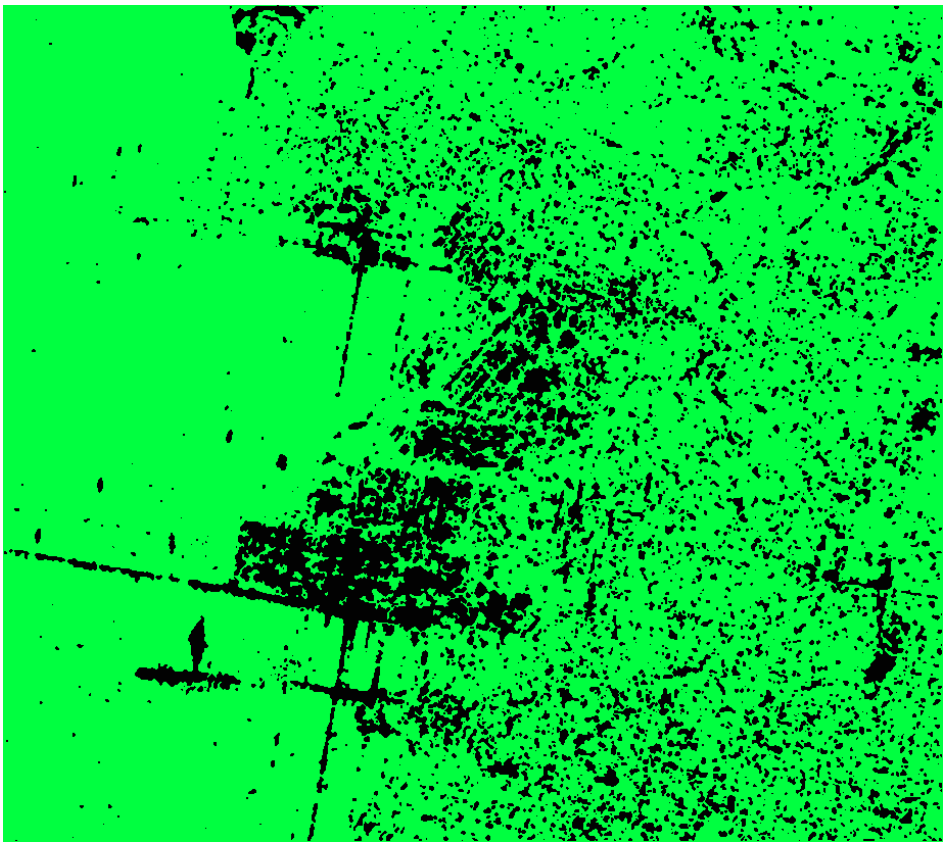

2^{nd} 4^{th} and 6^{th} order ratio image fusion

Once applied a significant number of filters, it's useless to apply more because all the information obtained will be irrelevant.

However, despite the significant changes, the binomial filter it's the simplest filter of the mentioned in the previous chapters and, for this reason, the less accurate of them.

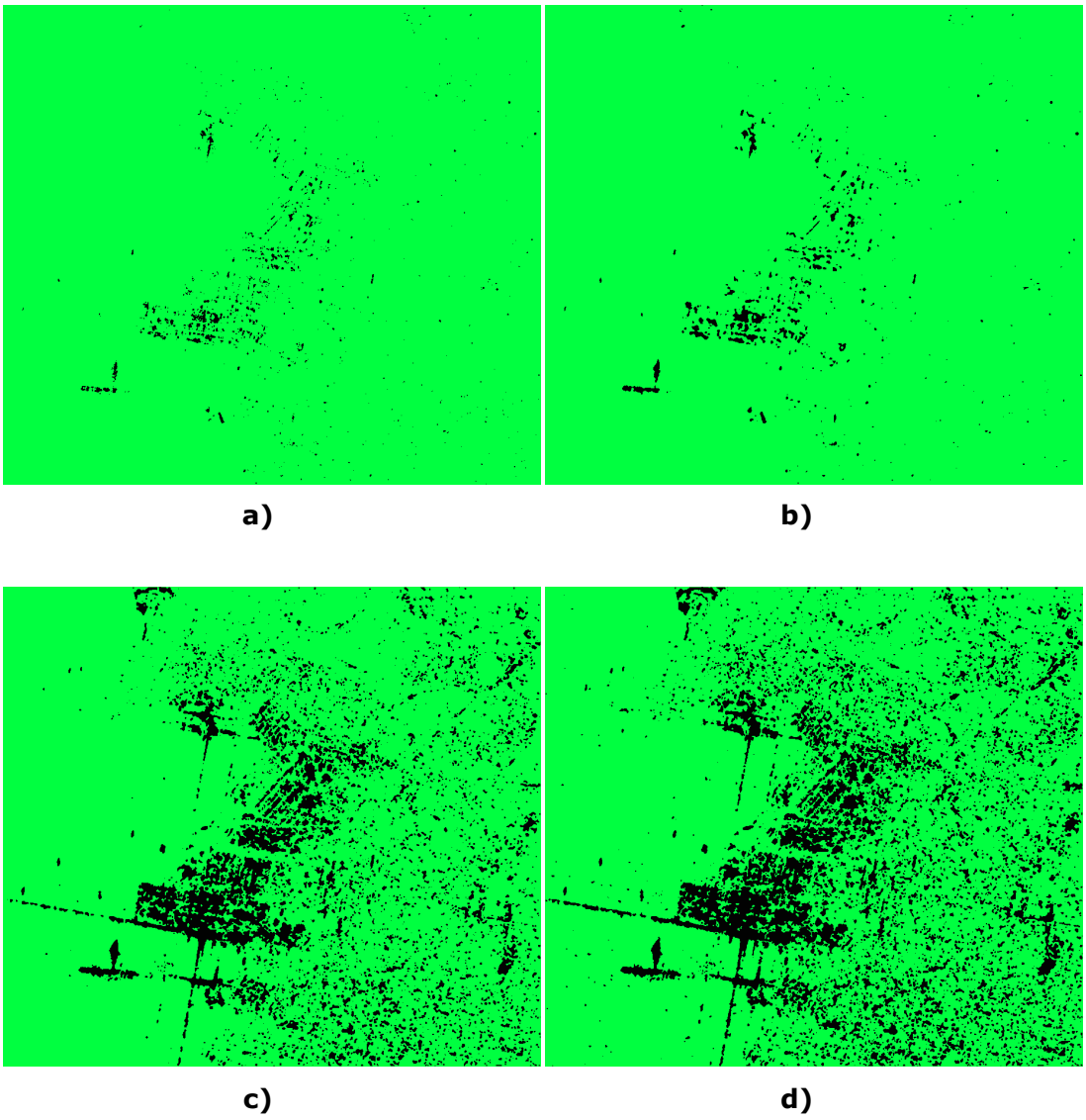

Fig.4: Comparison between the final image without filtering **a)**, with a 4^{th} order filtering **b)**, with a 2^{nd} and 4^{th} order ratio image fusion (plus the original) **c)** and a 2^{nd} 4^{th} and 6^{th} order fusion **d)**.

DWT EXPERIMENTAL RESULTS

The wavelet filtering implementation (both for discrete and stationary wavelets) it's a little bit more confusing due they are implemented in two different code languages. The whole process consists in the next steps:

- *Obtain the ratio image*: Obtain it using C++ and transform it to a format easier to read for matlab i.e: ".tif".
- *Filter the ratio image:* Filter it using the *wavelet* function created with many levels as necessary and with the desired wavelet, obtaining the ratio images and including them in the C++ implementation of the wavelet filter.
- *Run the main program*: To finish, run the main program in C++ and wait for the results.

It's not an ideal method to implement the filter but it's less cost computational and it's quite a lot simpler to filter using matlab than C++. Maybe in the future could be C++ implemented.

All the examples will be executed with the wavelet db-4 (Daubechies) being that there isn't any specification in this case for the wavelet election.

In the next images will be analyzed the final results fusing the original ratio image with 1^{st}, 2^{nd}, and 3^{rd} level decomposition respectively and additively, which means in the 2^{nd} level will be included the 1^{st}, and in the 3^{rd} the 1^{st} and the 2^{nd} for the image fusion (Fig.5).

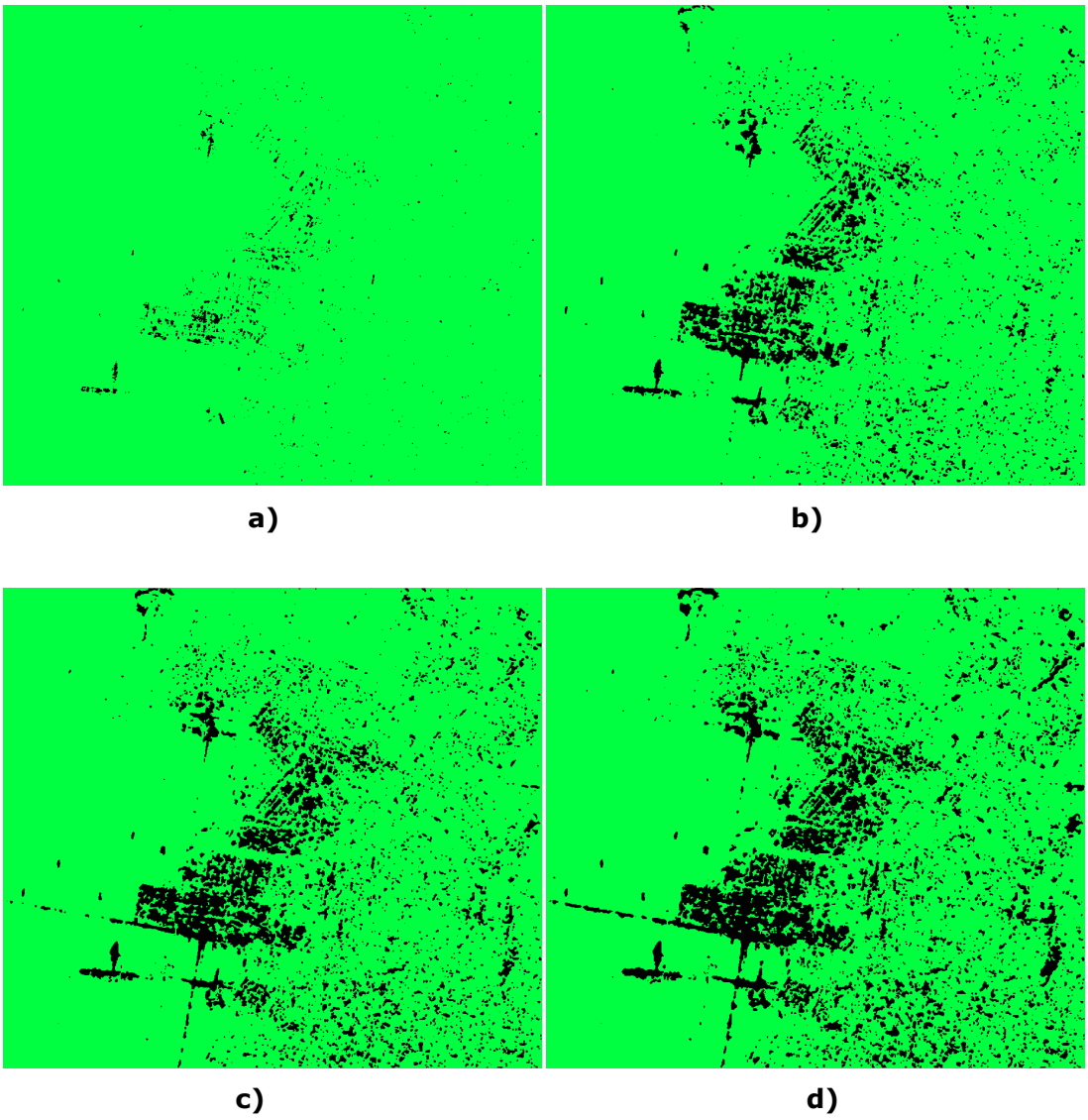

Fig.5: Comparison between the final image without filtering **a)**, with one level of DWT decomposition **b)**, with 2 levels of decomposition **c)** and with three levels **d)** (knowing all the previous levels are fused with the original ratio image).

SWT EXPERIMENTAL RESULTS

As did in the DWT method, SWT will be implemented in both C++ and matlab. The wavelet used will be db-4 as well (Fig.6).

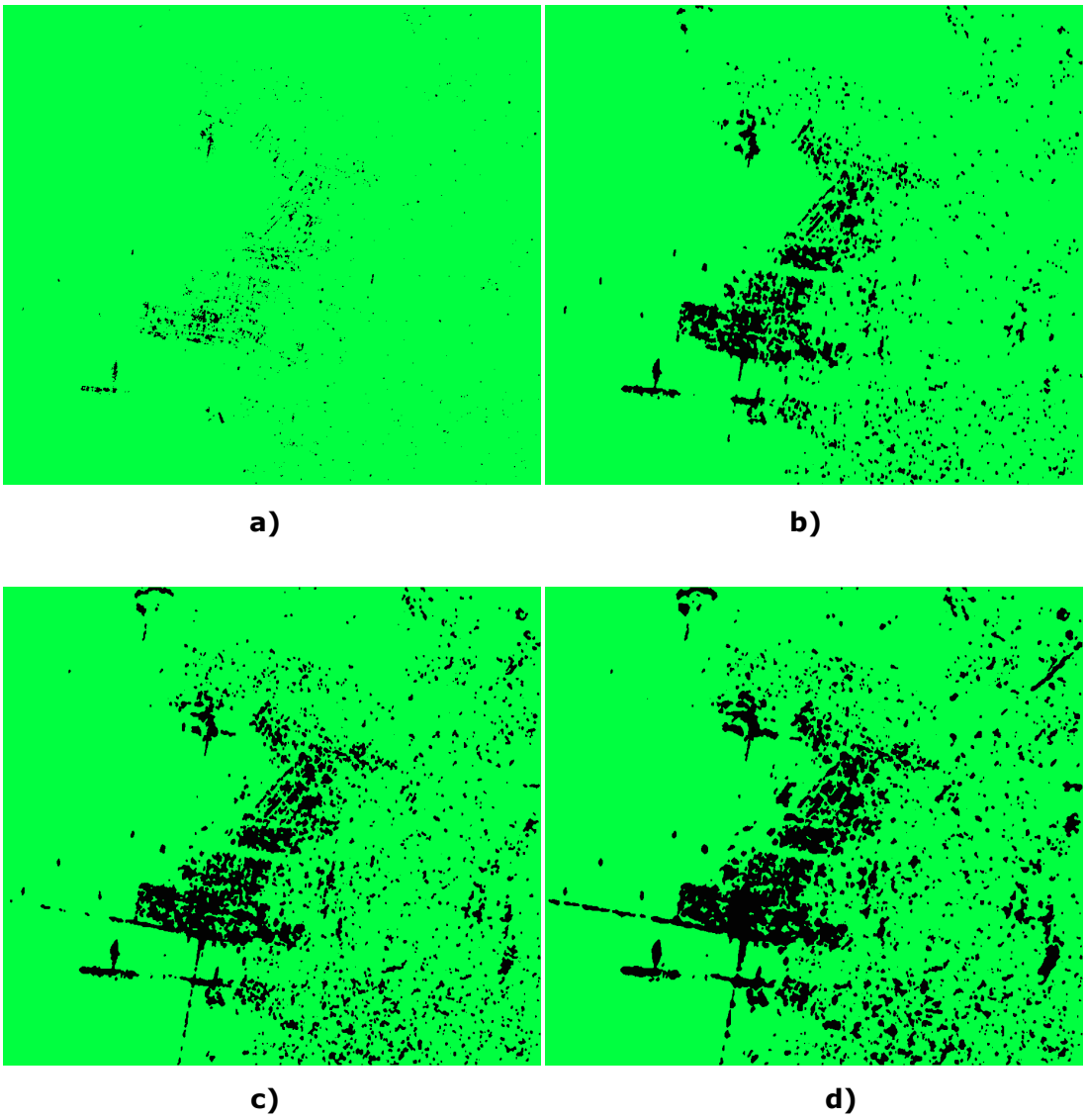

Fig.6: Comparison between the final image without filtering **a)**, with one level of SWT decomposition **b)**, with 2 levels of decomposition **c)** and with three levels **d)** (knowing all the previous levels are fused with the original ratio image).

As in the previous results, the change detection accuracy increases with each decomposition level.

DWT vs SWT

The election between the DWT and SWT transform will be based on the preferences wanted for the results.

If a quick and less accurate result is needed, the wavelet transform selected will be the SWT. This transform, as mentioned before, it's less cost computational but less accurate as well. This can be used in the case that a loss of information could be assumed. This loss is caused in the reconstruction of the image because the image is down-sampled in the decomposition.

For more efficient results the SWT will be the selected tool. It's more cost computational but the results are more precise. In the SWT the image it's not down-sampled in the decomposition, though there is redundant information, the reconstruction is more accurate because all the decomposed images are of the same size.

It's easy to appreciate that the SWT results are more compact than the DWT ones.

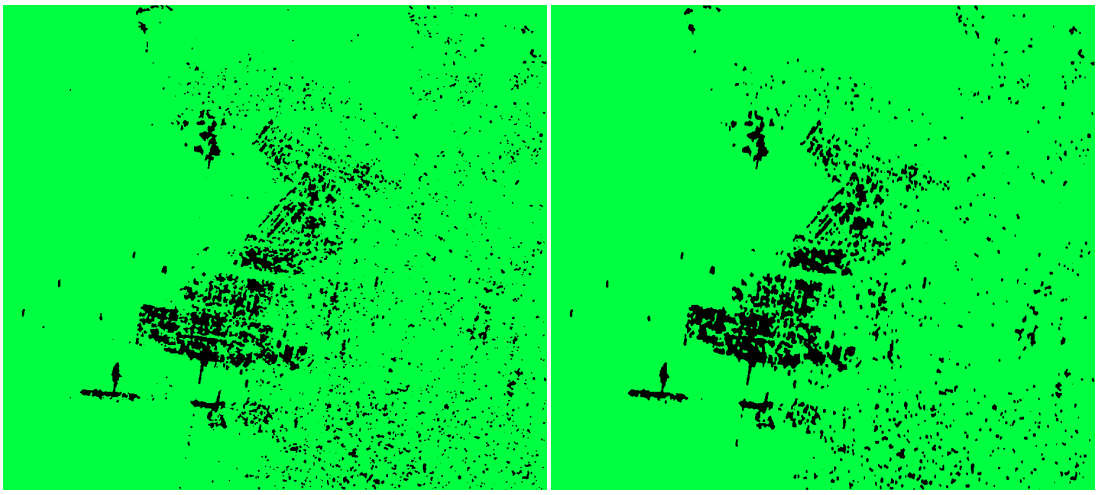

1st level decomposition; DWT (left) vs SWT (right).

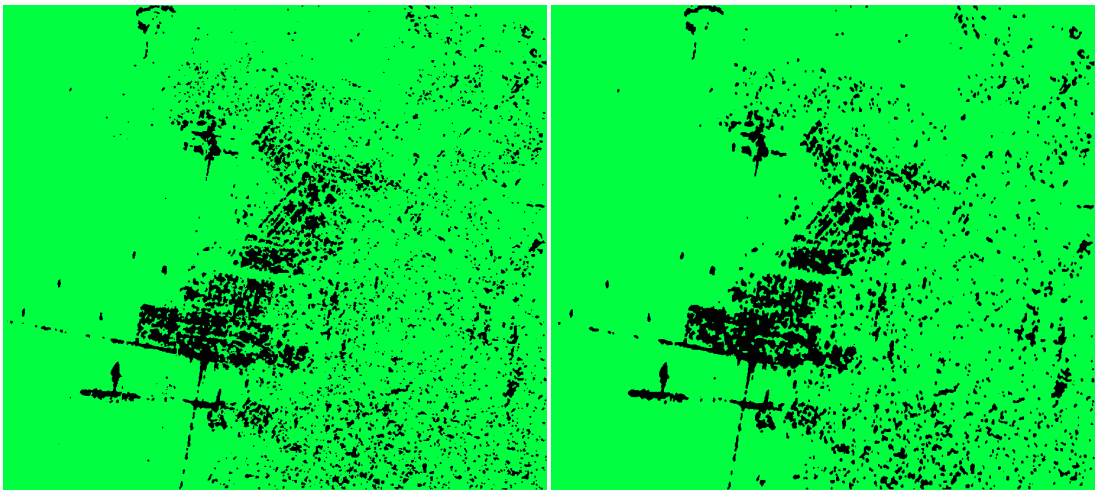

2nd level decomposition; DWT (left) vs SWT (right).

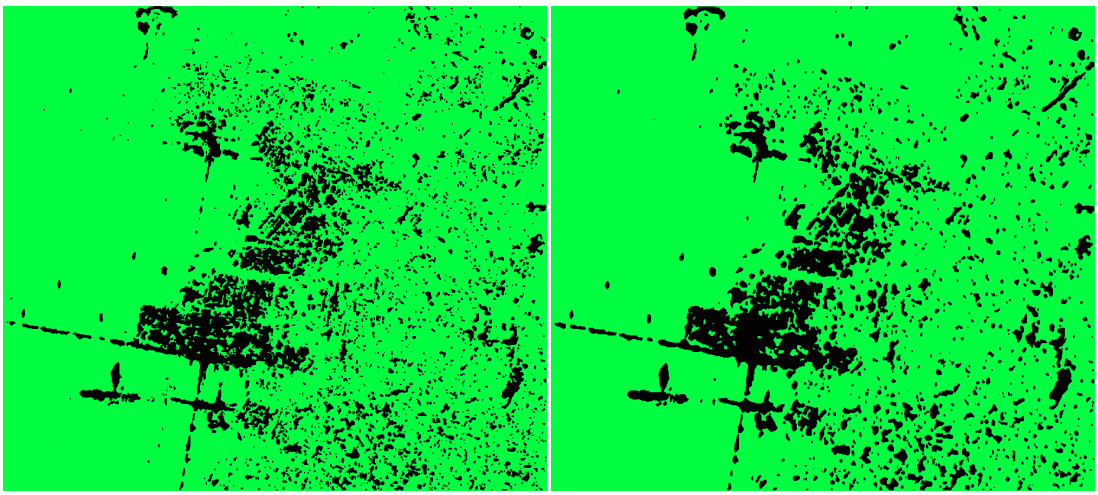

3rd level decomposition; DWT (left) vs SWT (right).

CONCLUSIONS

SUMMARY

There are many useful applications in remote sensing, like in this case multi-temporal change detection in SAR imagery. The objective of the method is to make change detection more effective and efficient in order to take full advantage of it. Change detection in multi-temporal SAR images it's not as accurate as expected. The proposed method improves the precision of the change detection, minimizing errors and increasing the change detection areas.

The method for change detection in multi-temporal imagery proposed, it's based on a generalized algorithm of the Kittler & Illingworth threshold (GKIT). The first part consists on generate a ratio image dividing, between them, each gray level pixel of the images. After that, one of the three versions of the GKIT (Nagakami-ratio, Log-normal and Weibull-ratio) is applied to the ratio image performing the change detection.

This algorithm, on his own, it's not enough to discriminate "change" areas from "no-change" areas with precision. In order to optimize the method three different filters have been developed. The first filter is a binomial filter, the second and the third are based on wavelets. One of the wavelet filters uses the discrete wavelet transform (DWT) and the other one the stationary wavelet transform (SWT).

The whole method described before, is implemented in both C++ and matlab. The C++ part is the main program (ratio operations and GKIT) and the binomial filter. Both, the wavelet filters are implemented in matlab, using the matlab wavelet tool box. When used the wavelet filter, it's necessary to, first create the ratio image in C++, then apply the filter in matlab and finally, with the filtered images, return to the C++ program to iniciate the change detection.

SUMMARY OF RESULTS

As mentioned in the experimental results part, the results are not cuantitative and must be interpreted by an observer. The results, of each one of the filter methods applied are satisfactory and the improvements obvius.

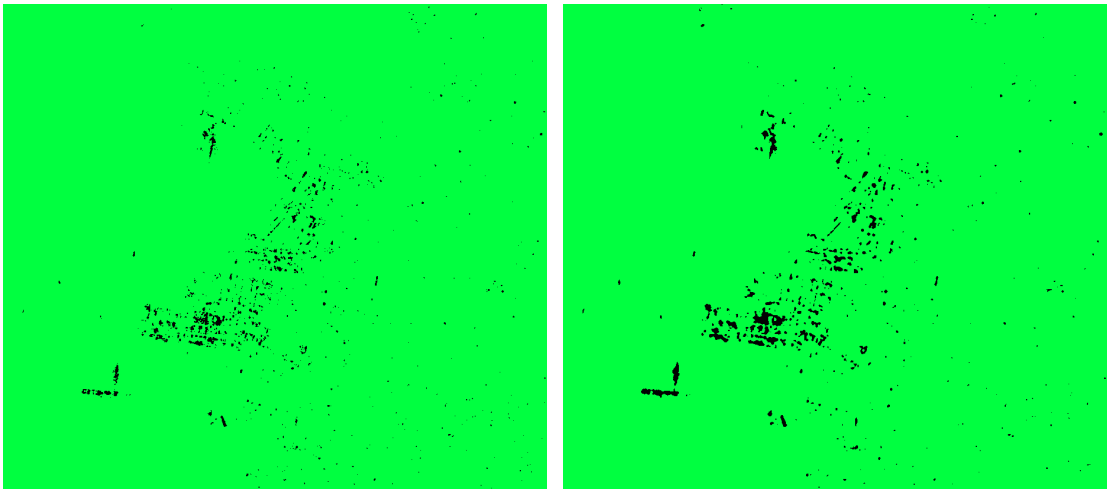

Fig.1: comparison between the final image without any filtering and the final image with a 4th order binomial filter applied to the ratio image, the differences are minimun.

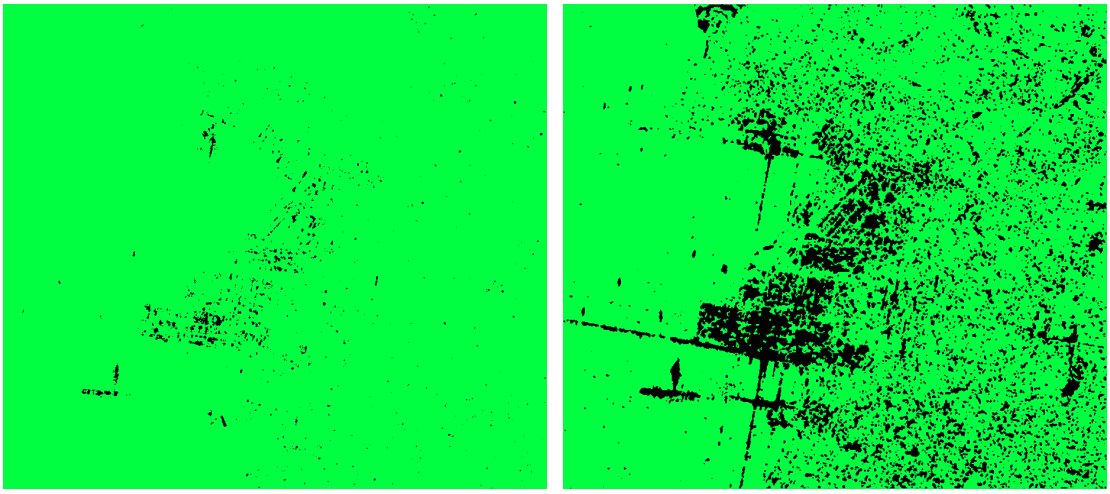

Fig.2: Comparison with a 2nd 4th and 6th level order binomial filtered ratio images plus the original. The "change" zones are more and more clear than in the previous comparison, but as a drawback, it has lot of "change" zones that are noise and could have misclassified.

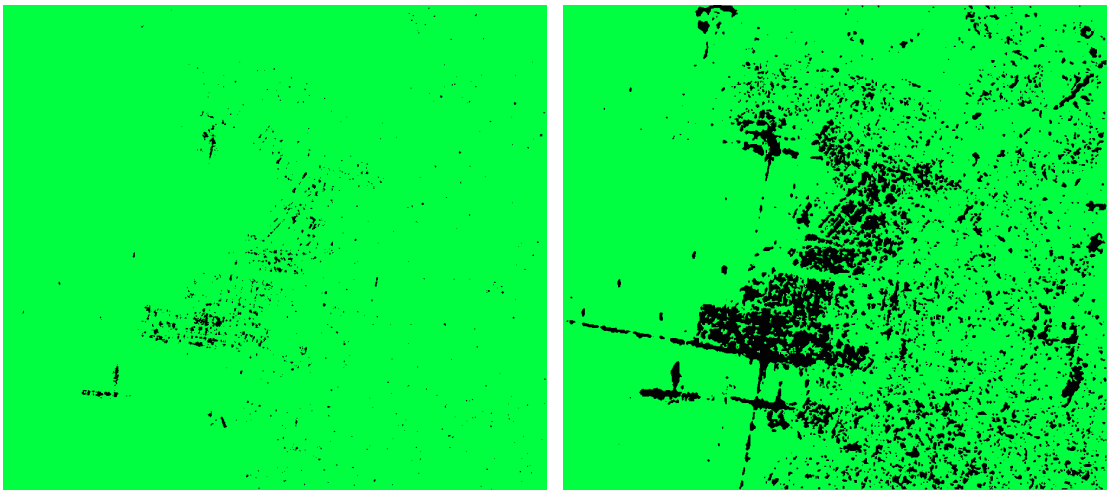

Fig.3: Another comparison, this time between the DWT filtering. Using a 3rd level decomposition and fusing with all the previous levels with the original ratio image the results are more compact but still there's some noise that could be not "change" zones.

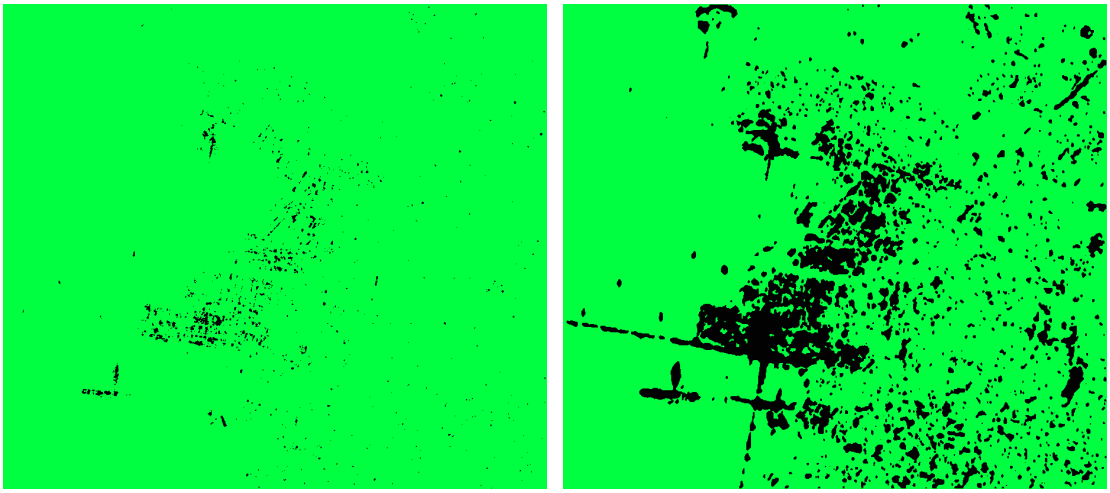

Fig.4: The last comparison between the image without any filtering and the SWT filtering. As in the previous comparison, 3rd level decomposition and fusion with the previous levels and the original ratio image is used. The results are more compact and it's probably the most accurate result of all of them.

FUTURE DEVELOPMENTS

Despite all the positive results, the method it's not refined yet, it could (and must) support future developments and improvements in order to take full advantage of it. In the following list there are many of the main drawbacks and improvemets that could be found:

- Two code languages: It's the main problem of the whole method. Changing between two code languages it's not efficient and in some cases could be a big loss of time. Although in matlab it's easier to implement the wavelet filters, in future developments, the whole program, including wavelet filters, will be implemented in C++. With this improvement it's eliminated the gap in the code that prevents to execute the whole program in one run. Could be maybe more cost computational, but the time reduction, and specially the over-work of the programmer/user, are considerably reduced.

- SWT: Another important drawback is the decomposition level limit that could be encountered in the SWT filter code. The decomposition level is limited to 3 due to the image size. For bigger levels is necessary to resize the image adding as much lines and columns of zeros as needed and eliminate them after filtering. One possible solution is to predict, with another algorithm, the number of lines and columns in function of the decomposition level and add and remove them when it's needed. This part is implemented in matlab and, as said before, the first problem to solve it's the two-code drawback, then, performing the fix in matlab will be less than useless. Once implemented the filter in C++ maybe this limit it's eliminated or it's necessary to take a different approach. The better solution it's to assume that the decomposition level limit it's 3 in SWT (this decomposition level is more than enough for good results) until the filter it's C++ implemented.

- Different filters: There is not a real need of more filters, but could be an advantage a smart use of the wavelet filtering. This means, using the most adequate mother wavelet (daubechies, biorthogonal, symlets, etc…) for each case. The development of this idea will be very difficult because the results in some images could not depend on the choice of the wavelet type, but in others could be very important. The criterion for the choice

it's difficult to define and will depend on the image characteristics. This improvement could be arranged over time with observation of the images.

- Different areas detection: Though it has nothing to do with the present thesis, looking at the results it's logic to think that this filtering will be very useful (especially SWT) in the detection on different areas like, water, vegetation, buildings, etc… . As well could be used for other applications of interest. Obviously the implementation would be totally different but some parts of the code may be usable.

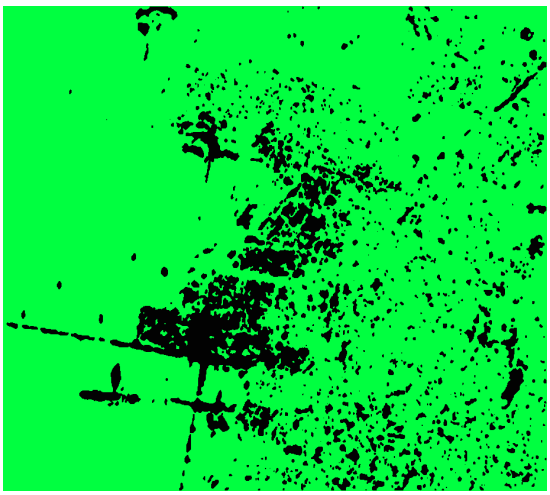

In the final image it's very easy to recognize the part of the port.

- Optimize: A topic in programming. Reducing the computational cost and execution time it's necessary and recommended in every code. Optimizing always brings efficient results and makes everything easier for the programmer/user. Would be necessary to optimize the parts in which these drawbacks are more relevant. Optimizing also includes writing the code in a way anyone who reads the code can easily understand it.

With the performance of this developments the final results would be even better than the obtained with the actual method.

References

[1] **Generalized Minimum-Error Thresholding for Unsupervised Change Detection From SAR Amplitude Imagery**; Gabriele Moser, *Member, IEEE*, and Sebastiano B. Serpico, *Senior Member, IEEE.*

[2] **A Markov Random Field Model for Classification of Multisource Satellite Imagery**; Anne H. Schistad Solberg, Member, IEEE, Torfinn Taxt, Member, IEEE, and Ani1 K. Jain, Fellow, IEEE

[3] **Wavelets for SAR Image Smoothing**; Graham Horgan

[4] **Unsupervised Change Detection from Multichannel SAR Data by Markov Random Fields**; Sebastiano B. Serpico and Gabriele Moser. University of Genoa, Dept. of Biophysical and Electronic Eng. (DIBE), I-16145 Genova, Italy, and Interuniversity Center of Research in Environmental Monitoring (CIMA), I-17100 Savona.

[5] **The Expectation Maximization Algorithm A short tutorial**; Sean Borman

Annex 1-The Expectation-Maximization Algorithm

The EM algorithm is an efficient iterative procedure to compute the Maximum Likelihood (ML) estimate in the presence of missing or hidden data. In ML estimation, we wish to estimate the model parameter(s) for which the observed data are the most likely.

Each iteration of the EM algorithm consists of two processes: The E-step, and the M-step. In the expectation, or E-step, the missing data are estimated given the observed data and current estimate of the model parameters. This is achieved using the conditional expectation, explaining the choice of terminology. In the M-step, the likelihood function is maximized under the assumption that the missing data are known. The estimate of the missing data from the E-step are used in lieu of the actual missing data.

Convergence is assured since the algorithm is guaranteed to increase the likelihood at each iteration.

The convergence properties of the EM algorithm are discussed in detail by McLachlan and Krishnan. Recall that θ_{n+1} is the estimate for θ which maximizes the difference $\Delta\ \theta\ \theta_n$. Starting with the current estimate for θ, that is, θ_n we had that $\Delta\ \theta\ \theta_n\ = 0$. Since θ_{n+1} is chosen to maximize $\Delta\ \theta\ \theta_n$, we then have that $\Delta\ \theta_{n+1}\ \theta_n\ \geq \Delta\ \theta_n\ \theta_n$, so for each iteration the likelihood $L\ \theta$ is non-decreasing.

When the algorithm reaches a fixed point for some θ_n the value θ_n maximizes $l\ \theta\ \theta_n$. Since *L* and *l* are equal at θ_n if *L* and *l* are differentiable at θ_n, then θ_n must be a stationary point of *L*. The stationary point need not, however, be a local maximum. In McLachlan and Krishnan it is shown that it is possible for the algorithm to converge to local minima or saddle points in unusual cases.

Annex 2-Wavelet Families

There are a number of basic functions that can be used as the mother wavelet for Wavelet Transformation. Since the mother wavelet produces all wavelet functions used in the transformation through translation and scaling, it determines the characteristics of the resulting Wavelet Transform. Therefore, the details of the particular application should be taken into account and the appropriate mother wavelet should be chosen in order to use the Wavelet Transform effectively.

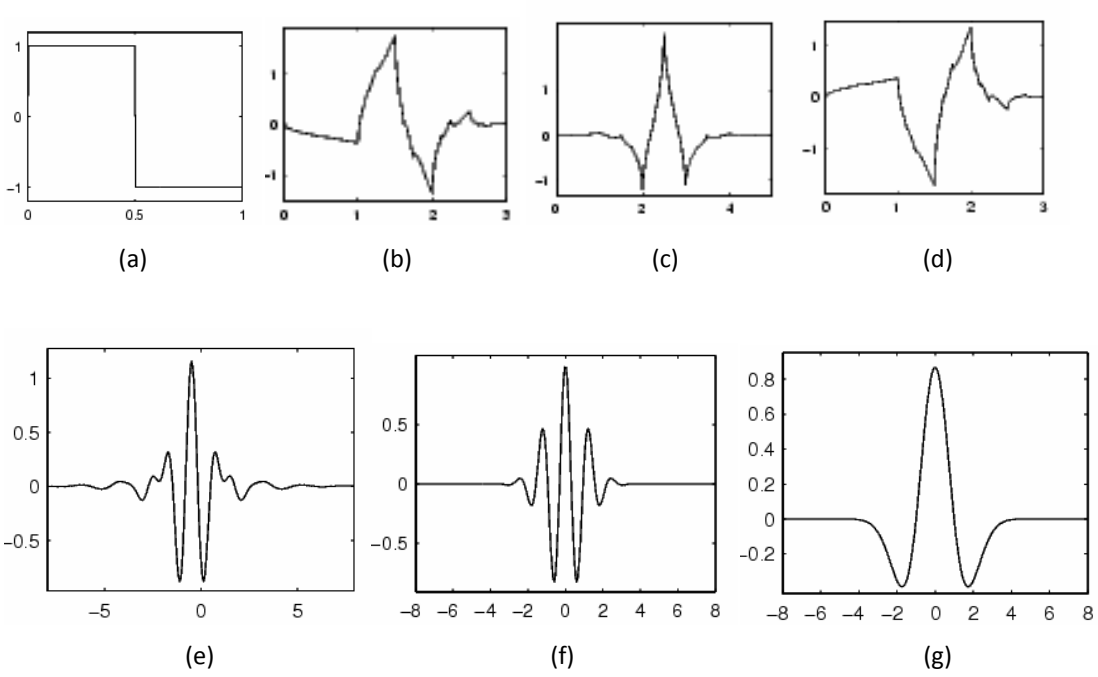

Wavelet families (a) Haar (b) Daubechies4 (c) Coiflet1 (d) Symlet2 (e) Meyer (f) Morlet (g) Mexican Hat.

This figure illustrate some of the commonly used wavelet functions. Haar wavelet is one of the oldest and simplest wavelet. Therefore, any discussion of wavelets starts with the Haar wavelet. Daubechies wavelets are the most popular wavelets. They represent the foundations of wavelet signal processing and are used in numerous applications. These are also called Maxflat wavelets as

their frequency responses have maximum flatness at frequencies 0 and π. This is a very desirable property in some applications. The Haar, Daubechies, Symlets and Coiflets are compactly supported orthogonal wavelets. These wavelets along with Meyer wavelets are capable of perfect reconstruction. The Meyer, Morlet and Mexican Hat wavelets are symmetric in shape. The wavelets are chosen based on their shape and their ability to analyze the signal in a particular application.